Ph.D. Course on *Vorticity, Vortical Flows and Vortex-Induced Vibrations*
Technical University of Denmark, Copenhagen, Denmark
vortex.compute.dtu.dk
August 26-30, 2019

Swirling Flow Instabilities: Pipes and Open Jets

Kerry Hourigan

Fluids Laboratory for Aeronautical and Industrial Research
Monash University, Melbourne, Australia
Otto Mønsted Guest Professor, Technical University of Denmark

MONASH University

FLAIR
Fluids Laboratory for Aeronautical and Industrial Research

Reading Material

Benjamin, T.B., Theory of the vortex breakdown phenomenom, J. Fluid Mech., 14, 593-629, 1962.

Billant, P., Chomaz, J.-M., and Huerre, P., Experimental study of vortex breakdown in swirling jets, *Journal of Fluid Mechanics*, 376, 183-219, 1998.

Dennis, D.J., Seraudie, C. & Poole, R. J., Controlling vortex breakdown in swirling pipe flows: Experiments and simulations, Phys. Fluids **26**, 053602, 2014.

Faler, J. H. & Leibovich, S., An experimental map of the internal structure of a vortex breakdown. J. Fluid Mech. 86 (2), 313–335, 1978.

Goldshtik, M. A., On swirling jets. Fluid Dyn. 14, 19–26, 1979.

Khalil, S., Hourigan, K. & Thompson, M.C., Effects of Axial Pulsing on Unconfined Vortex Breakdown, Physics of Fluids, 18, 038102, 2006.

Khoo, B. C., Yeo, K. S., Lim, D. F. & He, X., Vortex breakdown in an unconfined vortical flow. Exp. Therm. Fluid Sci. 14, 131–148, 1997.

Leibovich, S., The structure of vortex breakdown. Ann. Rev. Fluid Mech. 10, 221–246, 1978.

Mattner, T.W., Joubert, P.N. and Chong, M.S., Vortical flow. Part 2. Flow past a sphere in a constant-diameter pipe", J. Fluid Mech., 481, pp1-36, 2003.

Peckham, D. & Atkinson, S., Preliminary results of low speed wind tunnel tests on a gothic wing of aspect ratio 1.0, Royal Aircraft Establishment, 1957.

Sarpkaya, T., On stationary and travelling vortex breakdowns. J. Fluid Mech. 45 (3), 545–559, 1971.

Sarpkaya, T., Turbulent vortex breakdown. Phys. Fluids 7, 2301–2303, 1995.

Lecture Objectives

Learn:

The importance of vortex breakdown – aircraft, mixing chambers

The myriad of breakdown patterns found in ``open” flows

Some methods of controlling vortex breakdown

Controversial area

- Vortex breakdown has been a contentious area of fluid mechanics
- Theories fall into a number of different groups:
    - Near-axis boundary layer collapse
    - Internal flow separation
    - Inertial wave roll-up
    - Instability
    - Fold catastrophe

Overview

- **Motivation: Aircraft control, bioreactors**


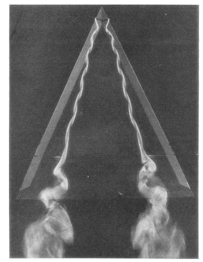


- **Vortex breakdown in open jets and pipes (cf closed cylinder)**

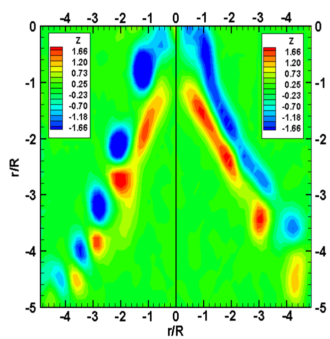

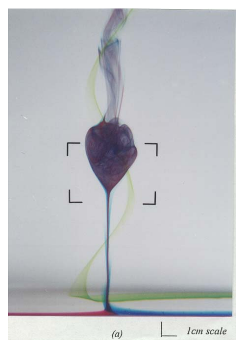

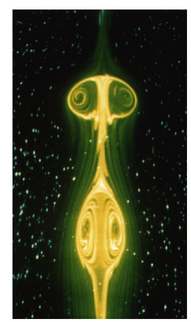

- **Control of vortex breakdown by pulsing and thermal effects**
- **Interaction between a bluff body (or a vortex ring) and a breakdown flow?**

Characteristics of VB

As the strength of the primary vortex steadily increases with angle of incidence or increase of swirl, bursting appears:

- rapid dilatation of the vortical structure
- profound alteration of its velocity
- occurrence of large-scale fluctuations

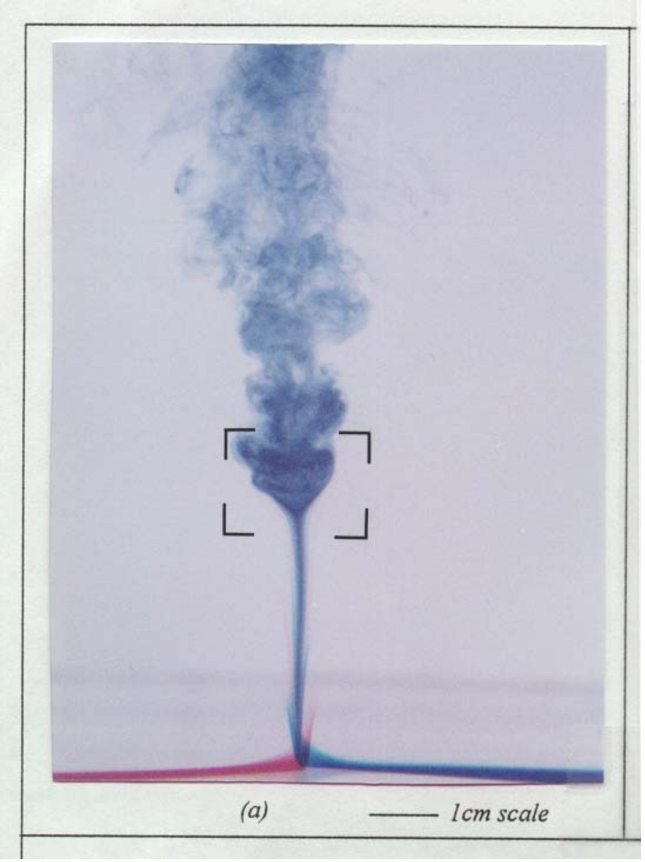

Different Types of Breakdown: Sarpkaya's 3 Classifications

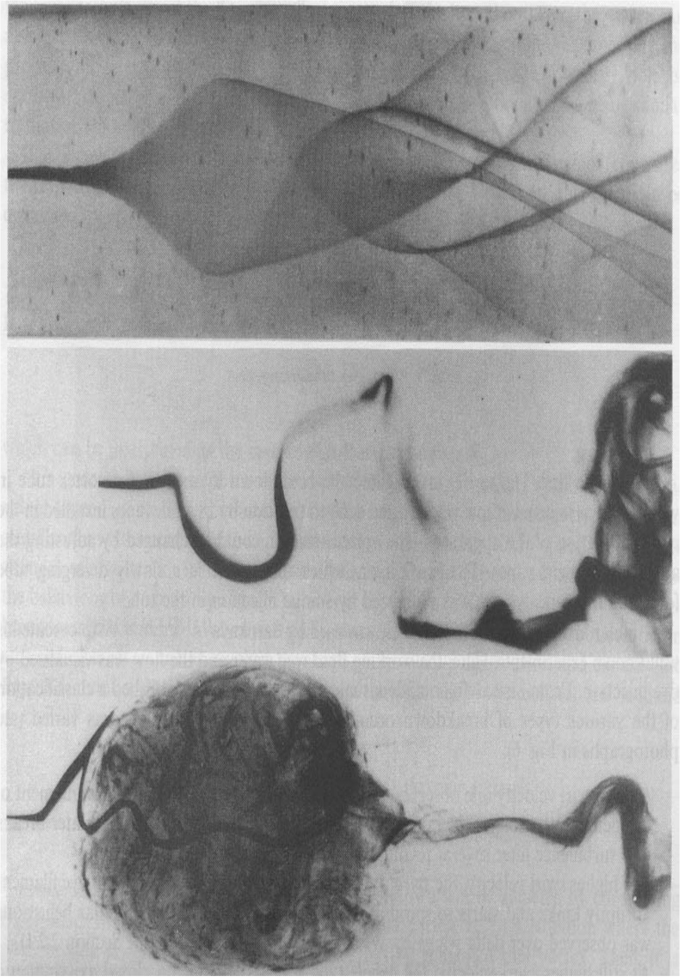

Double Helix: low swirl velocity

Spiral Type: higher swirl velocity

Bubble Type: still higher swirl velocity

The bubble type and the spiral type had been observed on delta wings; Sarpkaya observed the double helix.

Where is VB found?

- Highly swept wing or missile body at incidence
- Penetration of a jet in a transverse stream
- Flame stabilisation in combustion chambers
- Hydrocyclone separators
- Swirling jets behind nozzles
- Atmospheric vortices such as tornadoes

Fighter Aircraft

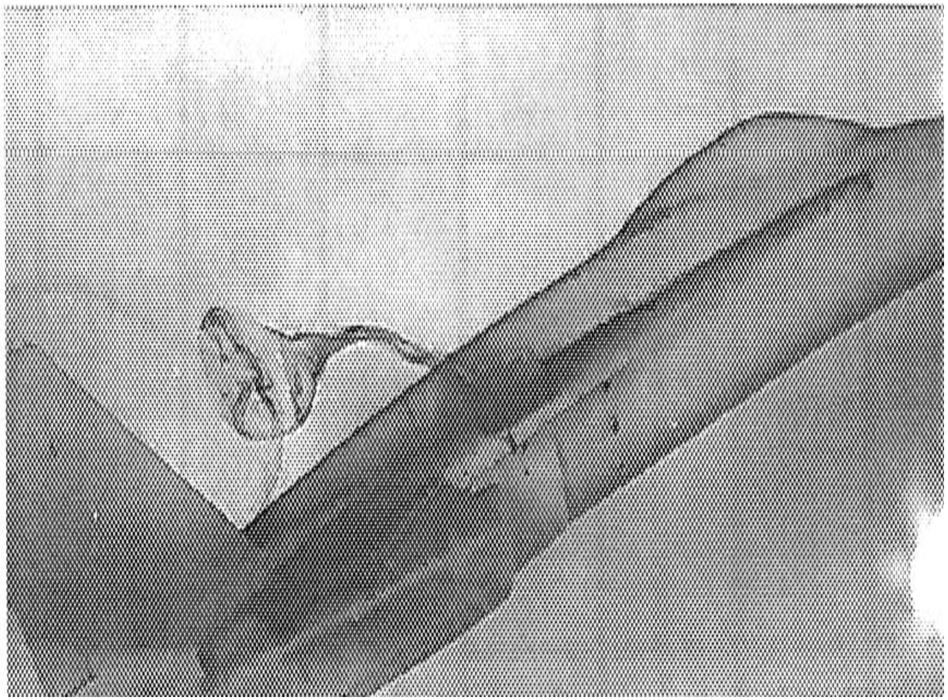

Water tunnel flow visualization of vortex breakdown over the F/A-18 (DSTO, 1990)

Flow over a Delta Wing

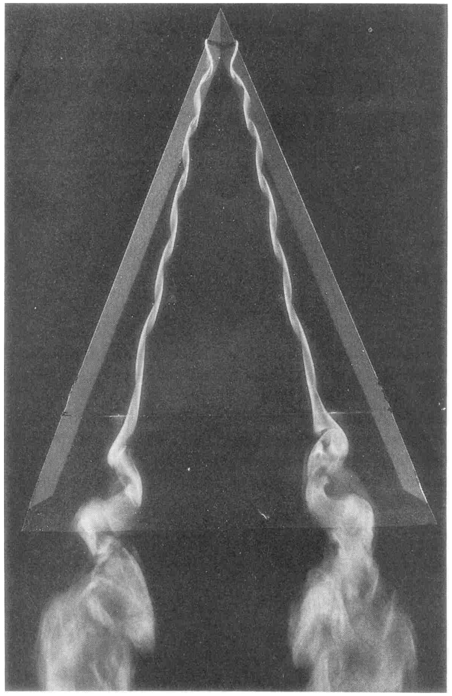

Water tunnel visualisation.
Delta wing with 65^0 sweep and 20^0 angle of incidence
(H. Werle (1971)

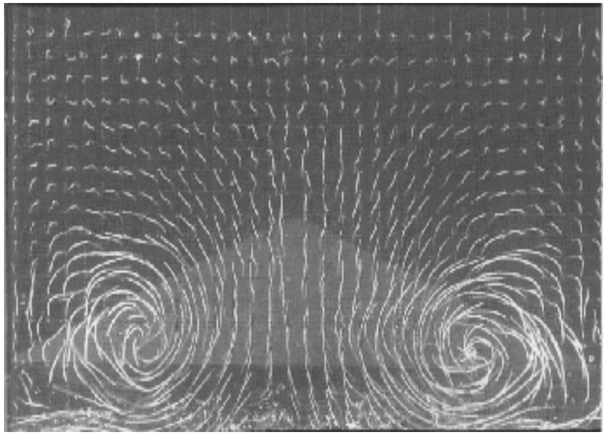

Pair of trailing vortices:tuft grid arranged behind the wing
(Fantasy of Flow, T. Tagori, The University of Tokyo)

Vortex Breakdown on a Delta Wing

www.youtube.com/watch?v=5_jt4x_TpOI

www.youtube.com/watch?v=S7V0awkweZc

Trailing Vortices

Boeing 747 at Kai Tak Hong Kong stirring up ground dust (World Engg, 15, 1996).

Classification System of Faler and Leibovich

Faler and Leibovich carried out experiments in an apparatus similar to Sarpkaya's and found 7 different flow disturbances (Type 1 is a variant of Type 0).

- Type 0 - "axisymmetric" bubble
- Type 1 - similar to Type 0, but with large-scale turbulence downstream of the bubble
- Type 2 - spiral type
- Type 3 - starts with a spiral and rapidly undergoes a disorganisation
- Type 4 - flattened bubble
- Type 5 - the dye departs from the structure centreline by staying in the meridian plane
- Type 6 - central filament moves gently off axis

Experiments of Khoo *et al.**

Khoo *et al.* undertook experiments in an "unconfined" chamber and found the 7 different flow disturbances plus an 8th (conical) breakdown.

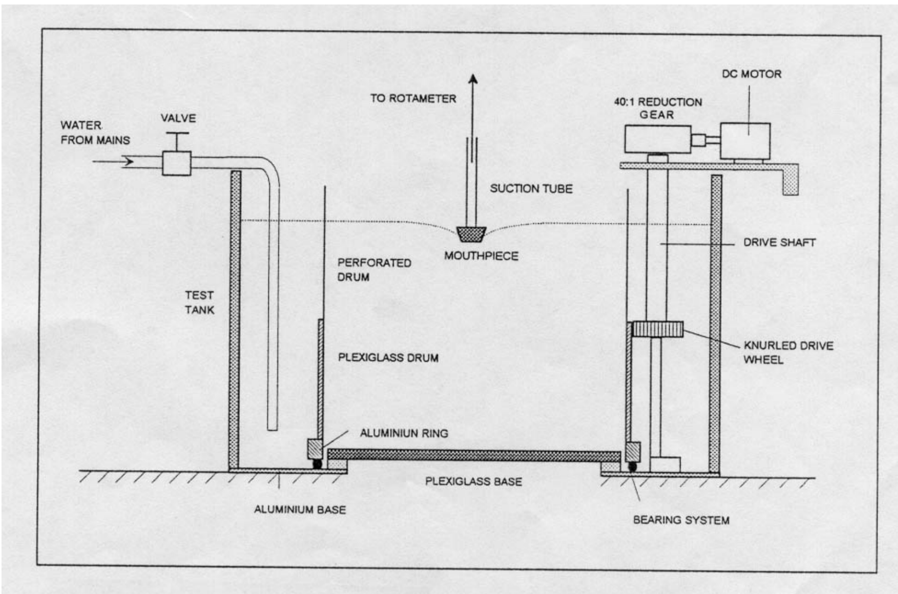

Reynolds no. $\mathbf{Re = V_0\, r_0 / \nu = \Gamma / 2 \pi \nu}$

Swirl no. $\mathbf{S = r_0\ \Gamma / 2 Q}$

where

Γ is circulation,

V_0 is tangential velocity at the drum radius r_0 , and

Q is suction flow rate.

*Khoo, B.C., Yeo, K.S., Lim, D.F. and He, X., Vortex breakdown in an unconfined vortical flow, Expt. Thermal and Fluid Sci., **14**, 131-148, 1997.

Breakdown Chart of Faler and Leibovich

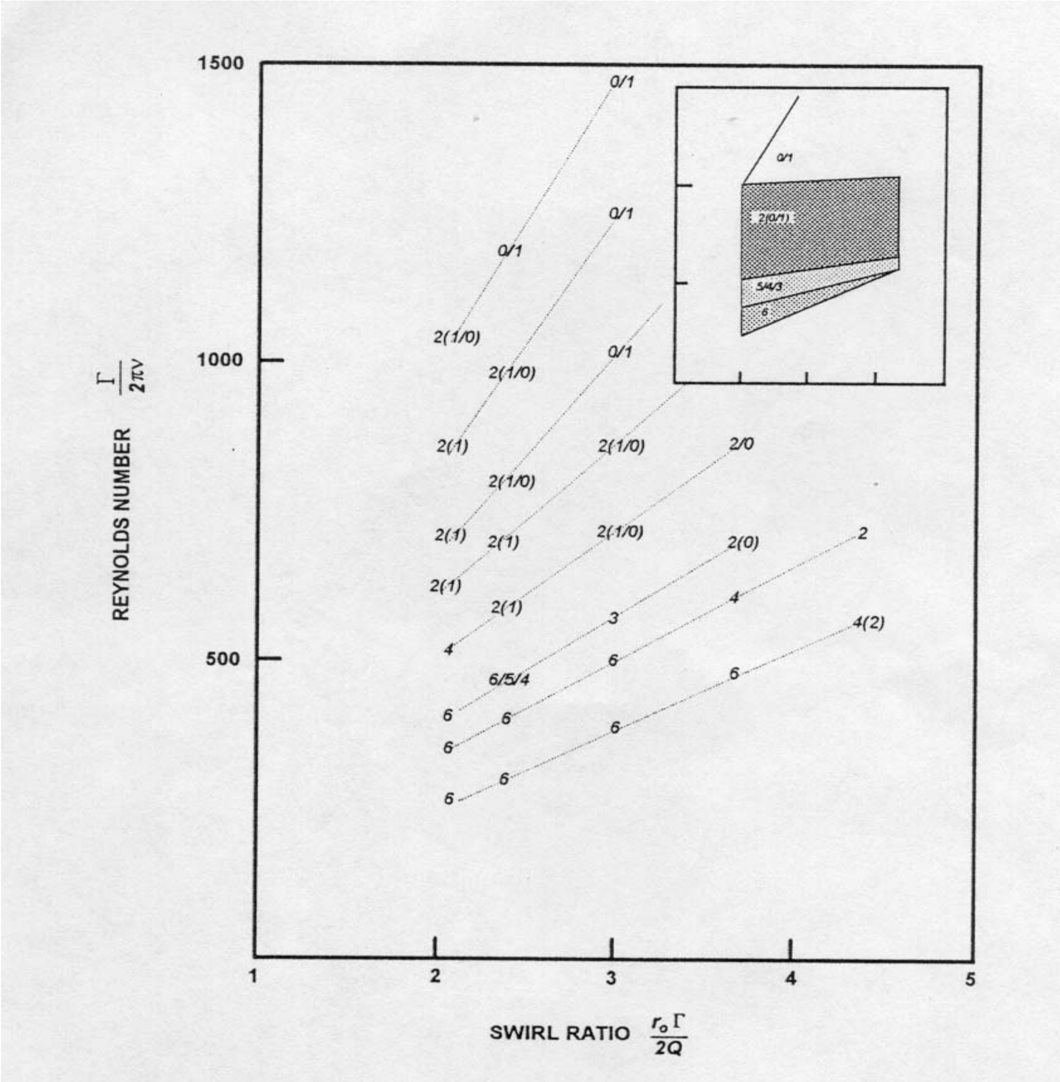

Breakdown Chart plotted using Re-S (insert indicates the region where each breakdown type is dominant)

Unconfined Breakdown Chart of Khoo *et al.*

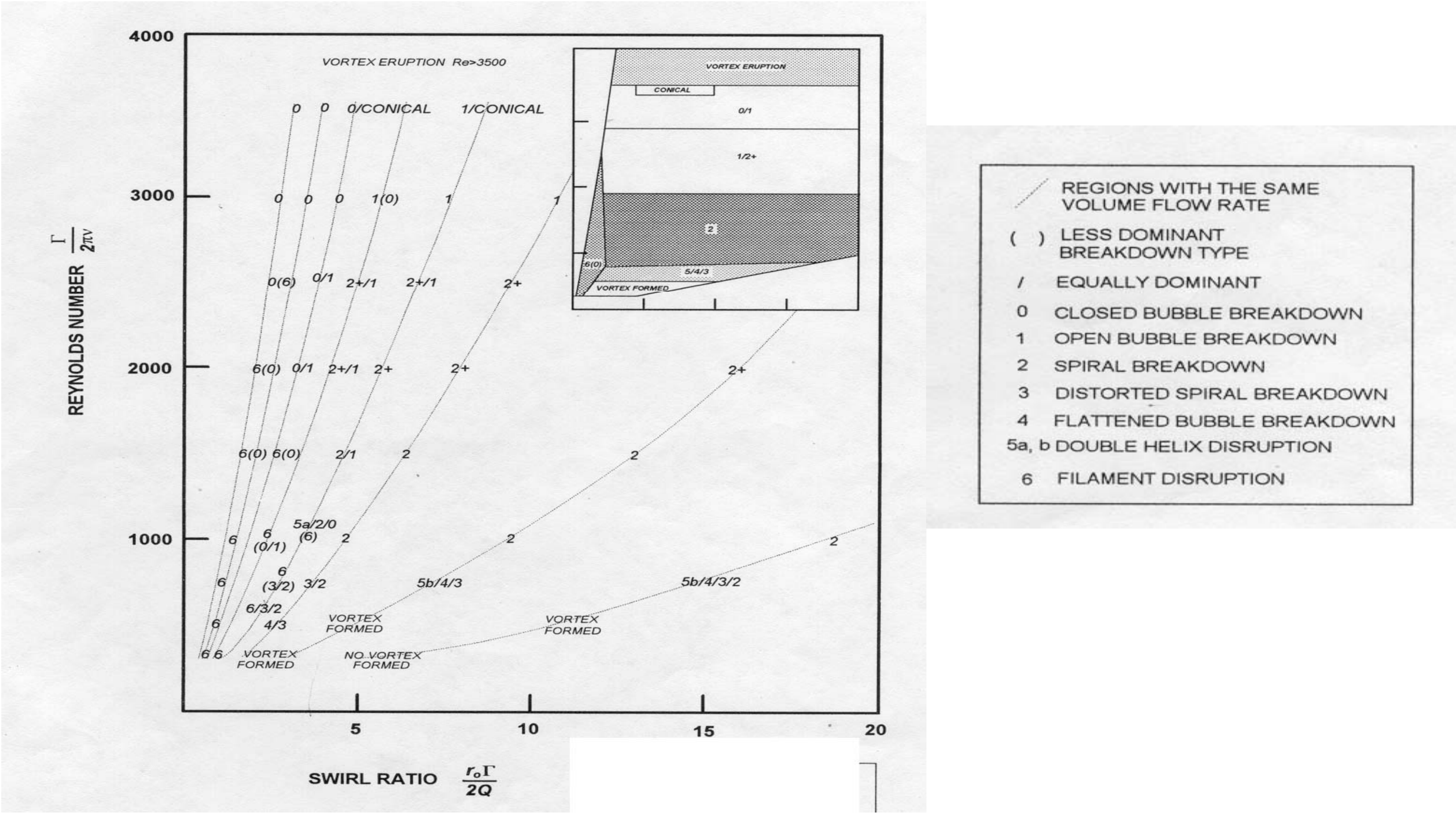

Unconfined Breakdown Chart Re vs S. Insert indicates region where each breakdown type is dominant

Generic Breakdown Chart

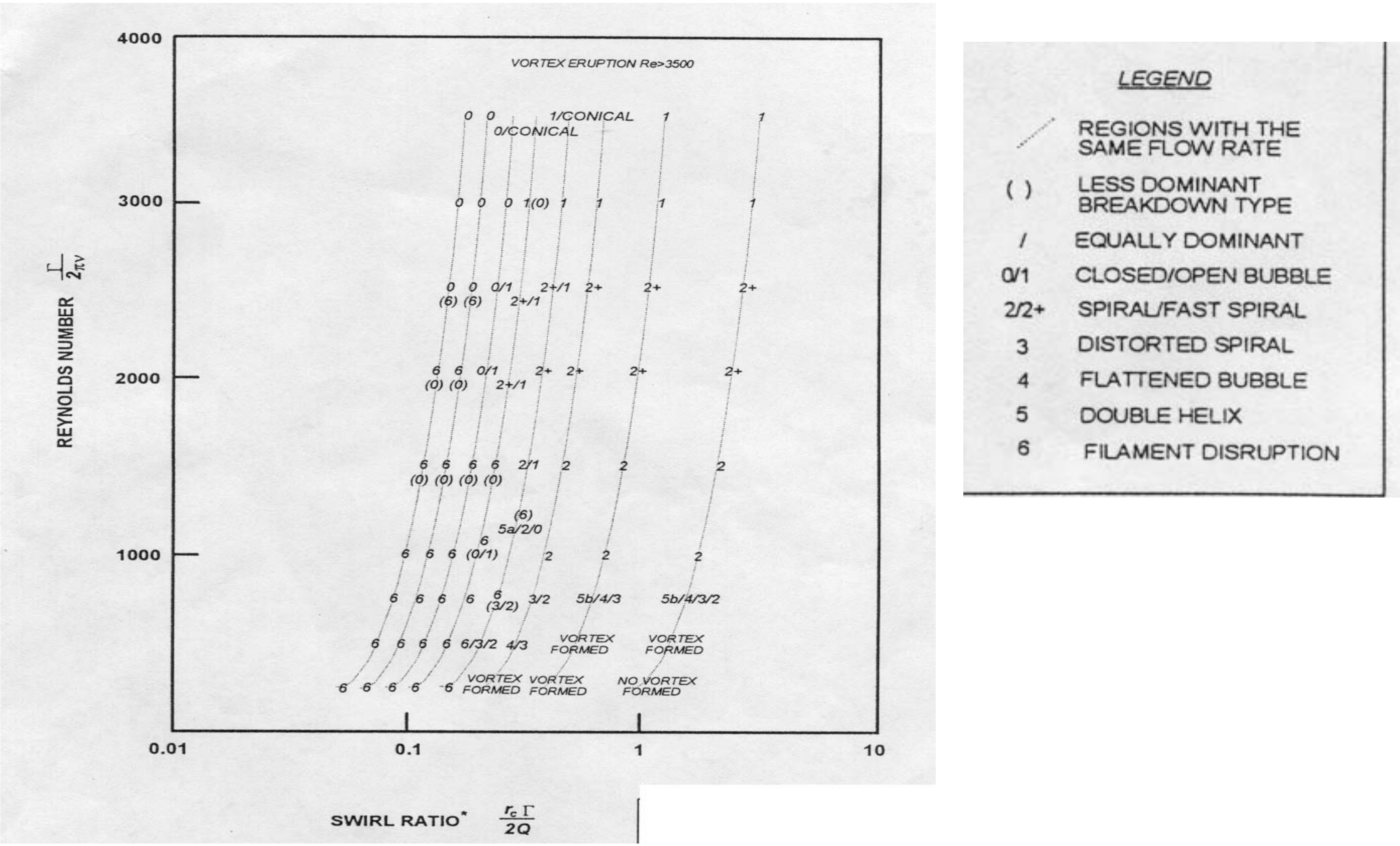

Generic Breakdown Chart Re vs S* with abscissa plotted in logarithmic scale

Experimental Rig: Faler & Leibovich

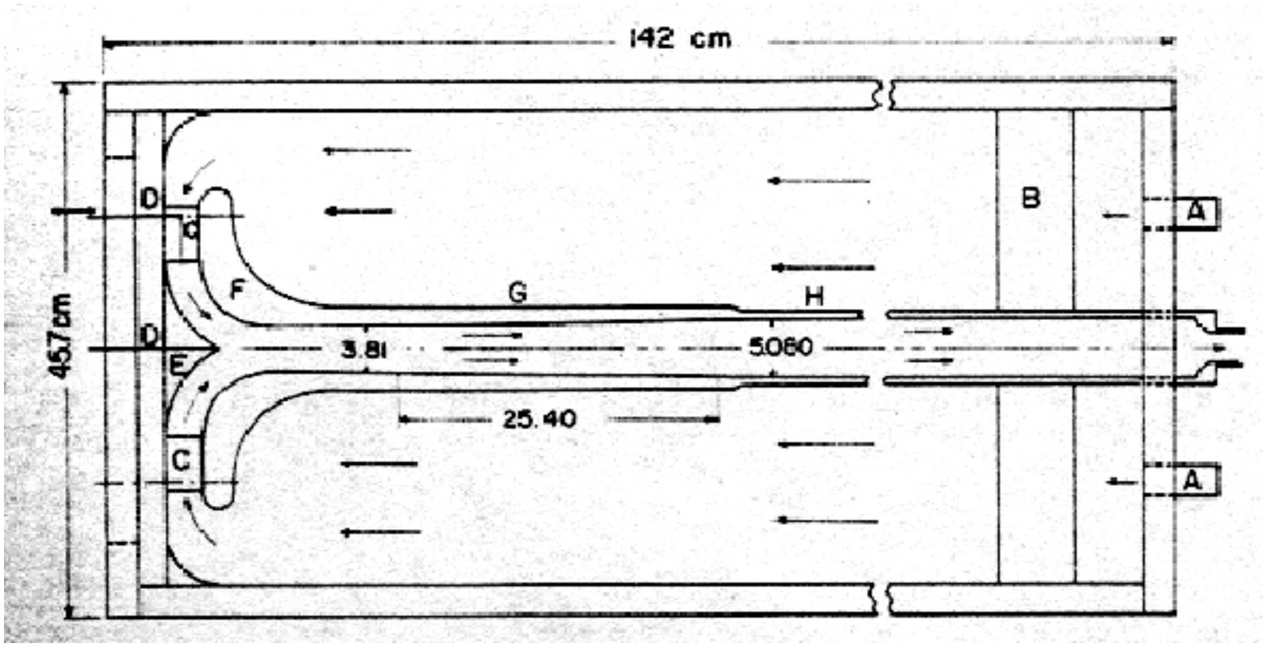

Test layout and dimensions. A. Inlet pipes (2 of 6 shown) B. Foam baffles C. Swirl vanes (2 of 32 shown) D. Dye injector tubes E. Centrebody F. Entrance channel bellmouth G. Test section H. Exit pipe

Pipe Flow

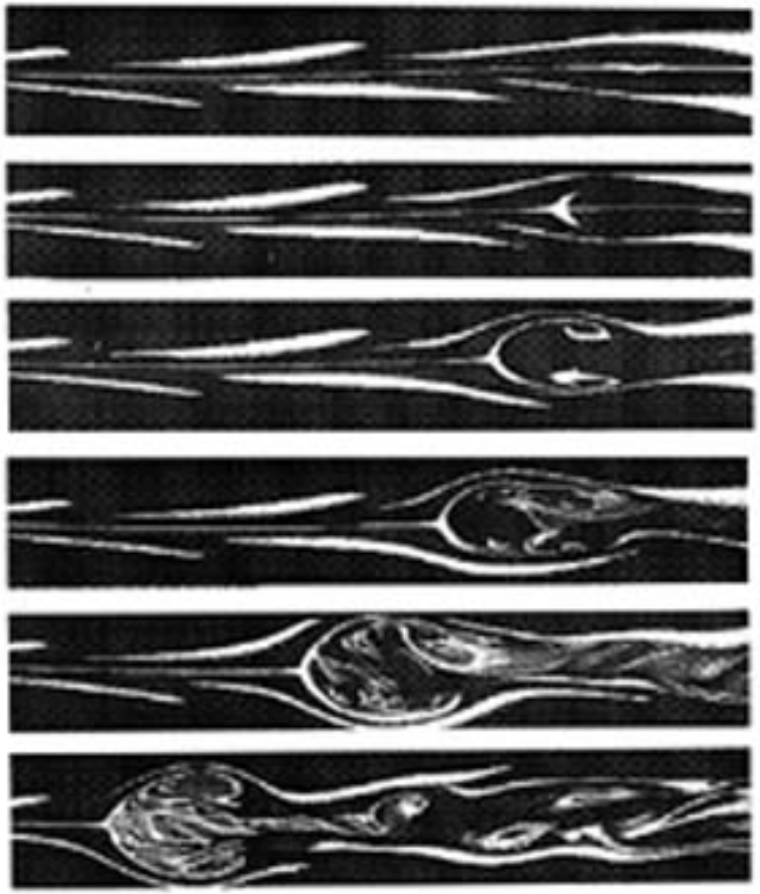

Escudier's (1986) observation of the formation and propagation of an axisymmetric (bubble type) vortex breakdown downstream of a guide-vane system (Re = 960).

Type 0 - Single-Tailed

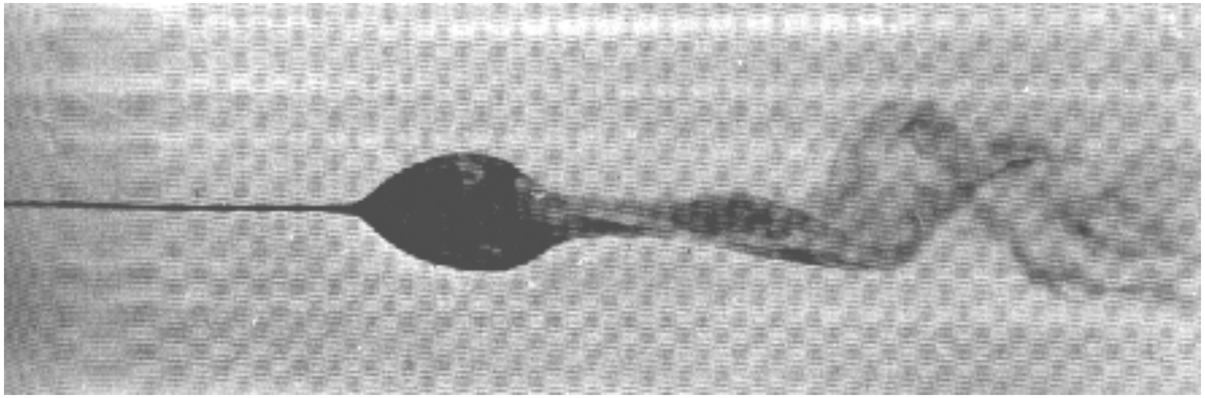

Type 0 (so-called axisymmetric) vortex breakdown.
Bubble shown is of single-tailed type (Re=2560, Ω=1.777).
Characterised by a stagnation point on swirl axis, followed by an abrupt expansion of the centreline dye filament to form the envelope of a bubble of recirculating fluid. The envelope has a high degree of axial symmetry over most of its length, but the rear is not closed and is asymmetrical.
The bubble was simultaneously filled and emptied at the rear portion, at diametrically opposite locatoins.

Type 0 (cont.)

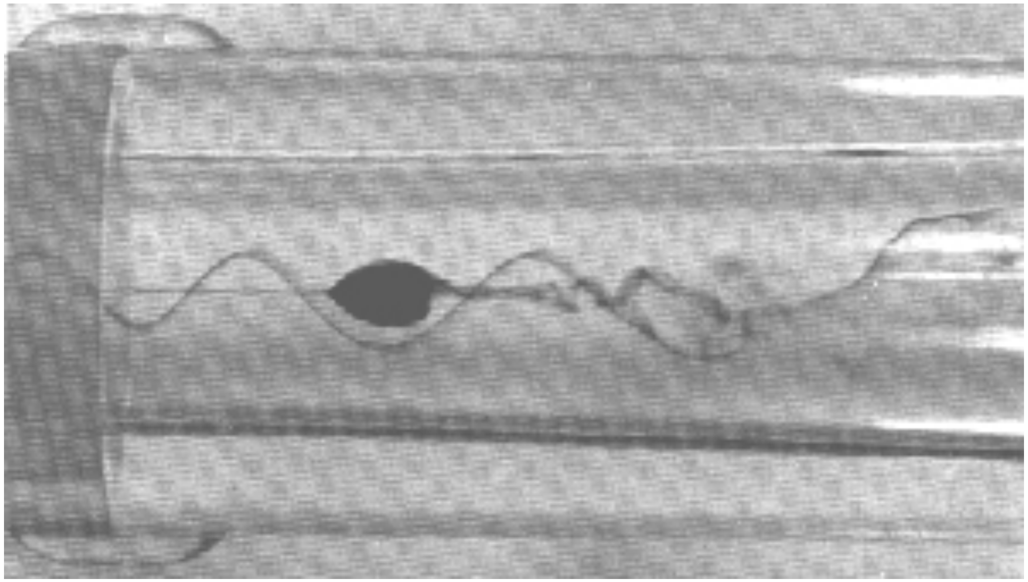

Type 0 vortex breakdown. Outer helical dye filament passes over breakdown without disturbance. A second disturbance (in this study always of the spiral Type 2) was nearly always evident approx. one bubble length downstream of the rear of the first breakdown.

Type 0 - Two-Tailed

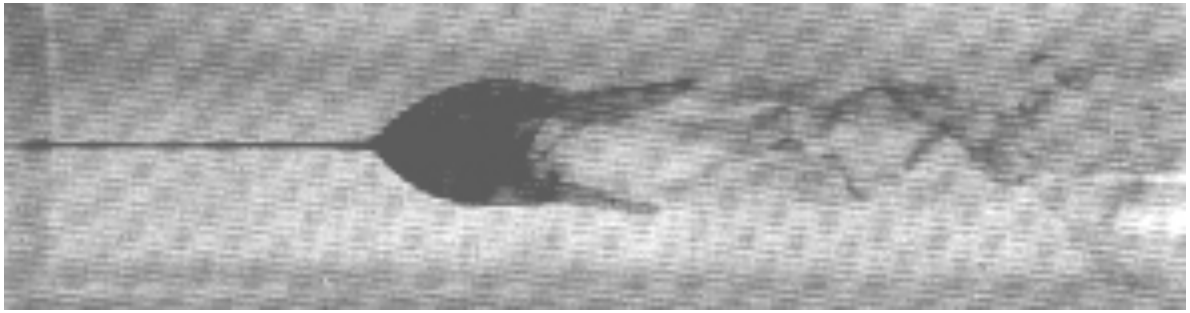

A two-tailed Type 0 vortex breakdown - as with the single-tailed bubble, the emptying tails rotated about the axis in a regular periodic fashion The filling points were diametrically opposed and 90^0 out-of-phase with the empting tails..

Type 0 - Worm-Screw Dye Filament

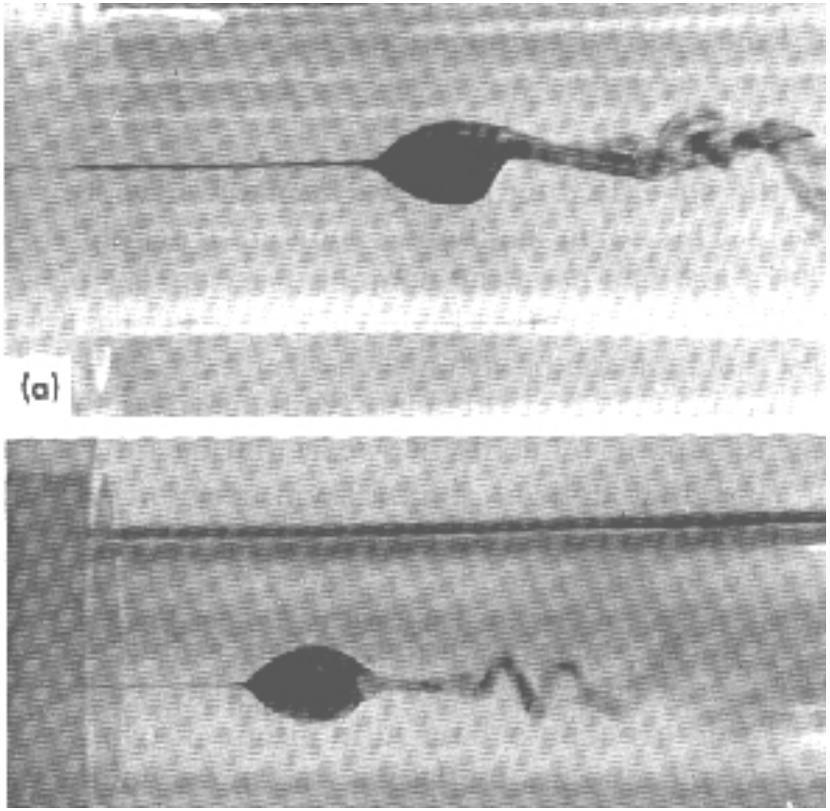

Type 0 breakdown with Re = 2560 (Upper) and Re = 4200 (Lower). Screw-worm dye filament was observed starting just downstream of the nose and fed from the darkened region near the nose; this screw-worm filament had the same sense of axial and swirl velocity as the base flow.

"Closed" Bubble

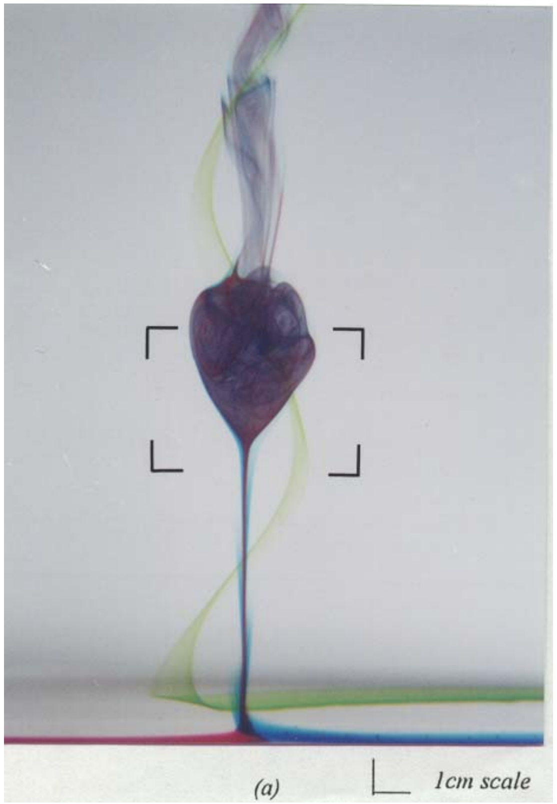

Re = 3000, S = 4.0
(Khoo *et al., 1997*)

Type 1

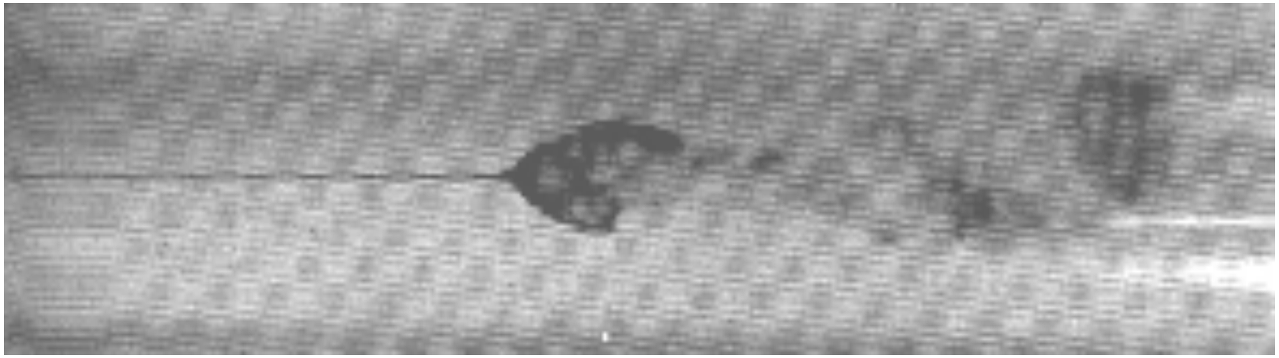

Type 1 breakdown:
Did not have the smooth envelope, distinct emptying tail, and clearly evident downstream vortex core displayed by Type 0. Nose region appeared slightly asymmetric

Type 1 breakdown alternated with Type 0. It would drift about its mean position randomly but travel upstream and eventually change abruptly into Type 0, which would drift downstream before changing suddenly into Type 1. Appears there were 2 quasi-equilibrium “potential energy valleys” separated by a “peak” which was only occasionally surmount.

Open Bubble Breakdown

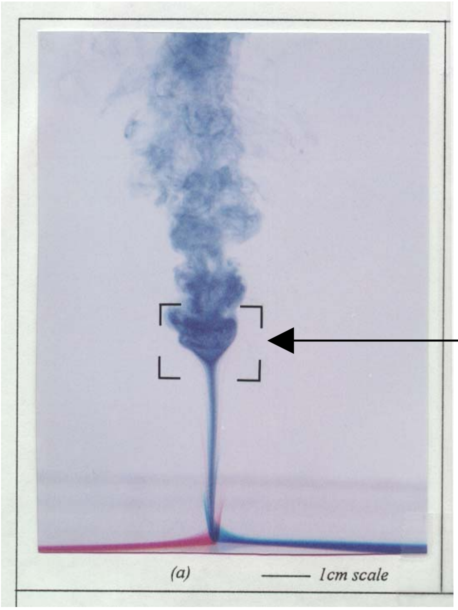

Re = 3000, S = 4.0
(Khoo *et al., 1997*)

Type 2

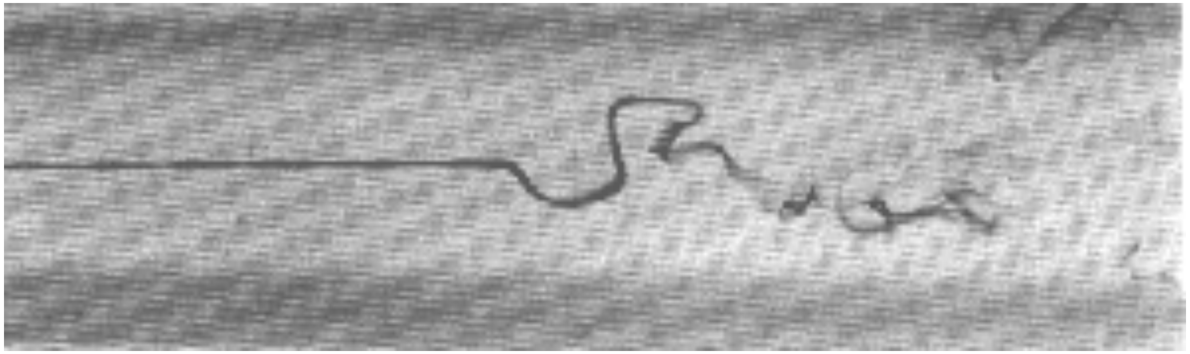

Type 2 spiral mode of vortex breakdown - this form is most commonly observed in the flow over delta wings at high angles of attack. The central dye filament decelerated rapidly and formed a spiral which persisted for 1 or 2 turns before breaking up into large-scale turbulence. Turns of the spiral had the same sense as the base flow and the whole spiral configuration rotated in a periodic fashion about the tube axis in the same direction as the base flow. The spiral also drifted axially.

For an increase in Re, (a) the mean axial location of the spiral moved upstream, (b) the maximum radius the the spiraling filament reached, before breaking up, decreased slightly, (c) frequency of rotation around the tube axis increased.

Spiral

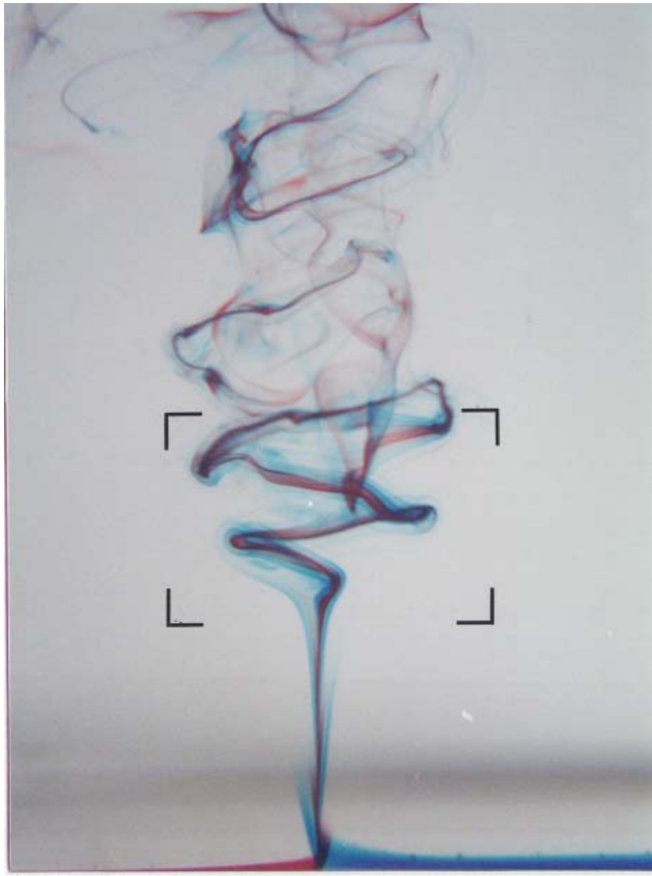

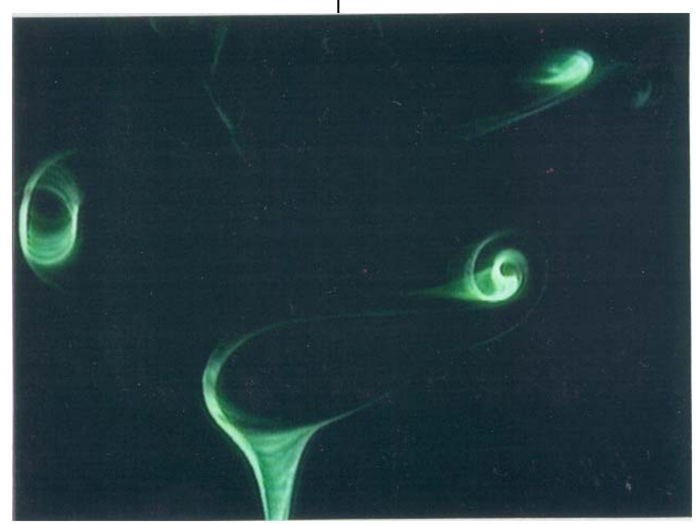

Re = 1000, S = 9.0. Note the distinct rolling-up of the vortex filament (Khoo *et al*., 1997).

Distorted Spiral

Re = 750, S = 7.5 (Khoo *et al.*).

Type 6

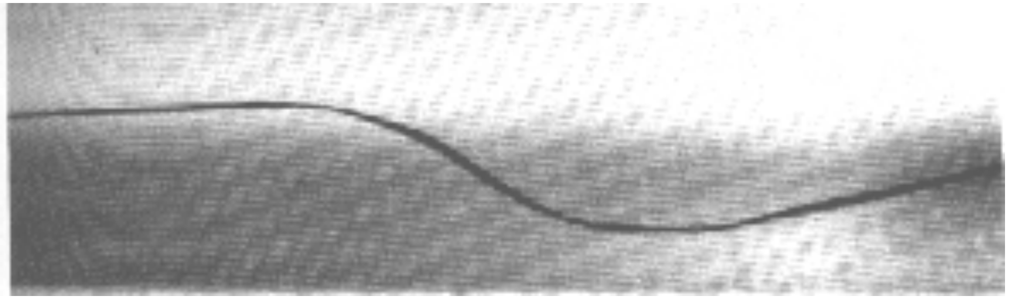

Further slight increases in swirl led to transition from Type 2 to **Type 6** disturbance in which central dye filament did not shear but only deflected off axis.

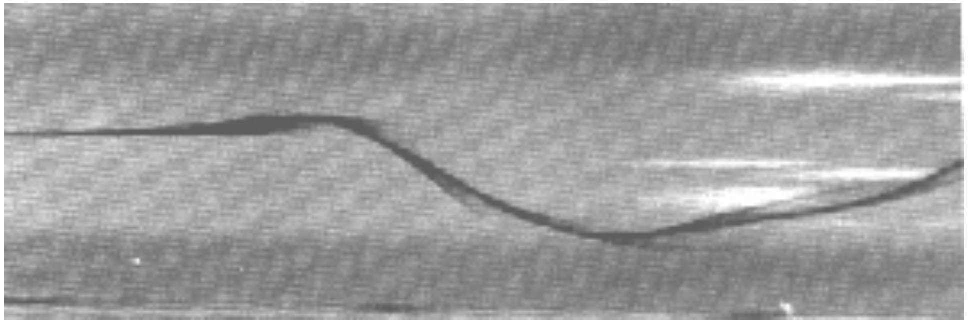

As swirl was increased, the tendency for the central filament to shear into a tape increased.

Filament Disruption

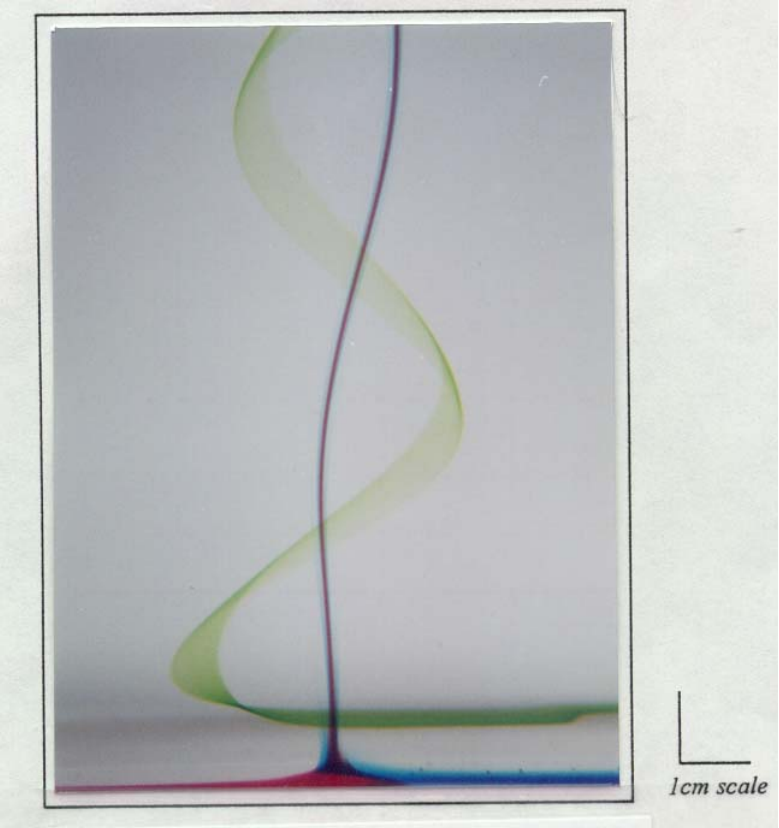

Re = 1000, S = 1.5 (Khoo *et al.*)

Type 5 - Double Helix

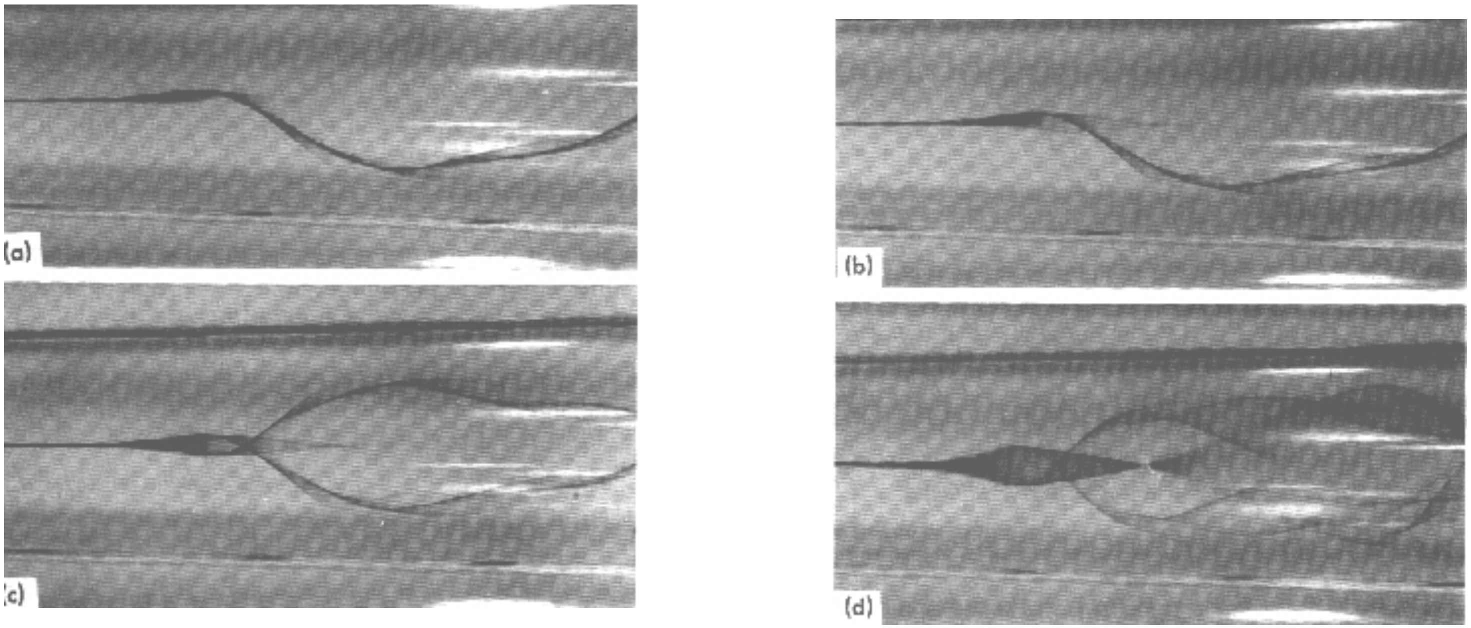

The evolution of the **Type 5** disturbance (first reported by Sarpkaya and referred to as a double helix) from Type 6 (above evolution over 5 mins). Once formed, pattern was steady in form and location. The central filament sheared, on axis, into an ever widening, triangular shaped sheet, with each half winding around the other until moving out nearly to reach the tube wall.

Double Helix

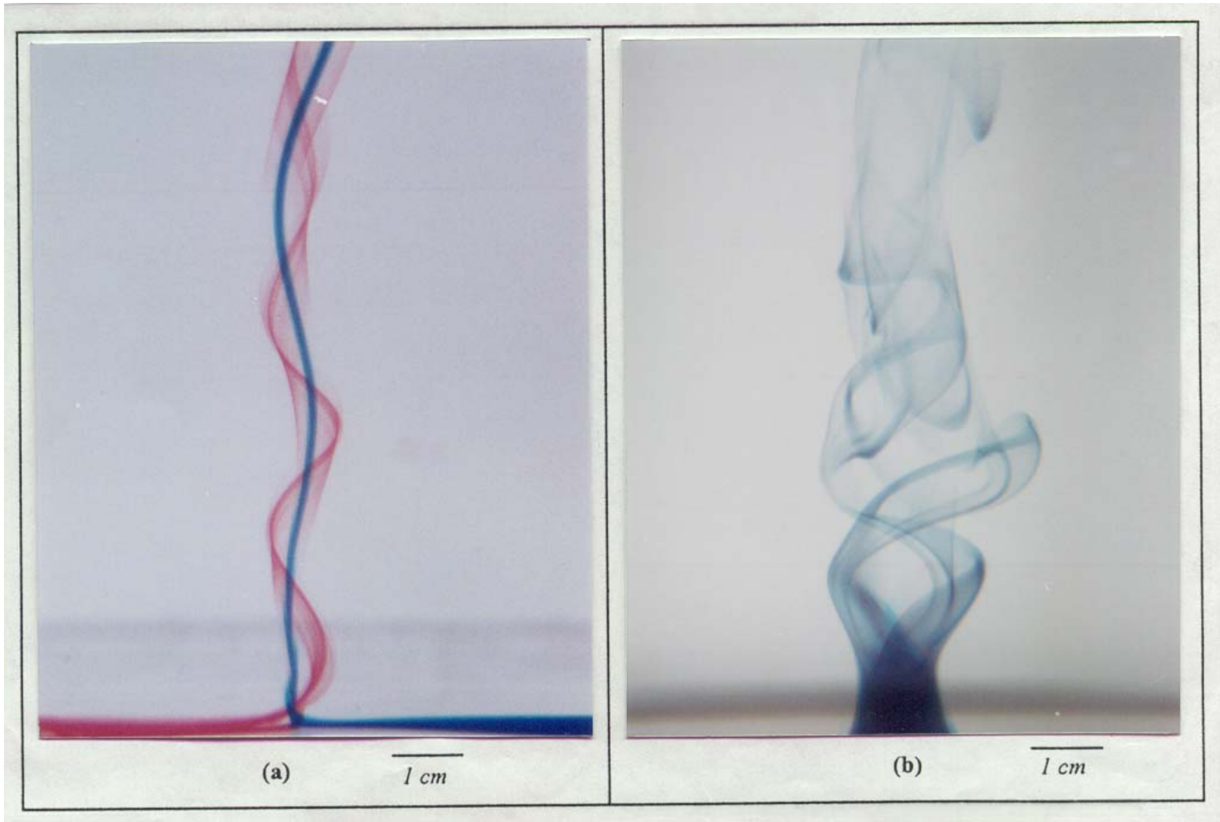

(a) First type in which helical filament arose from flow separation at the boundary layer, and (b) Second type in which the second spiraling filament arose from a kink formed on the effusing core (Khoo *et al.*).

Type 4

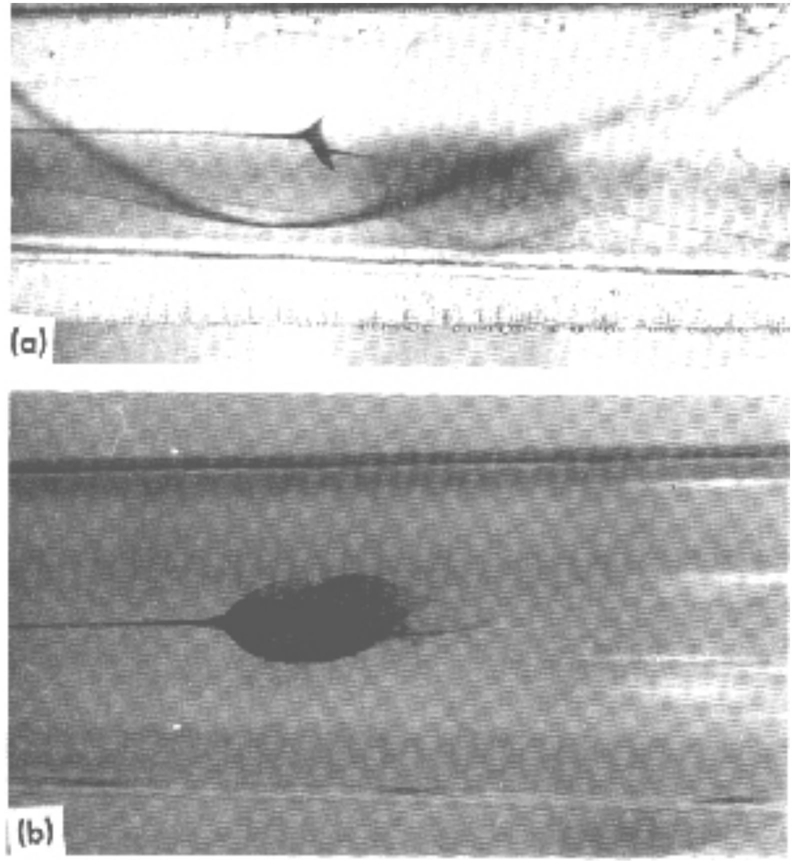

A partially formed **Type 4** disturbance. Type 4 usually evolved directly from Type 6, either spontaneously at fixed flow conditions or could be induced by slightly increasing the swirl.

Type 4 (cont.)

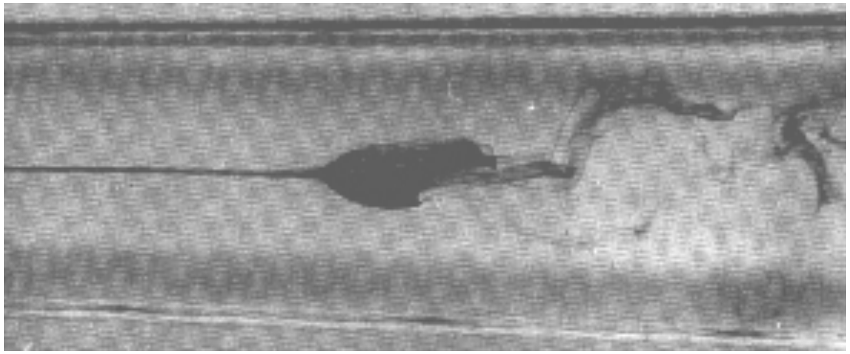

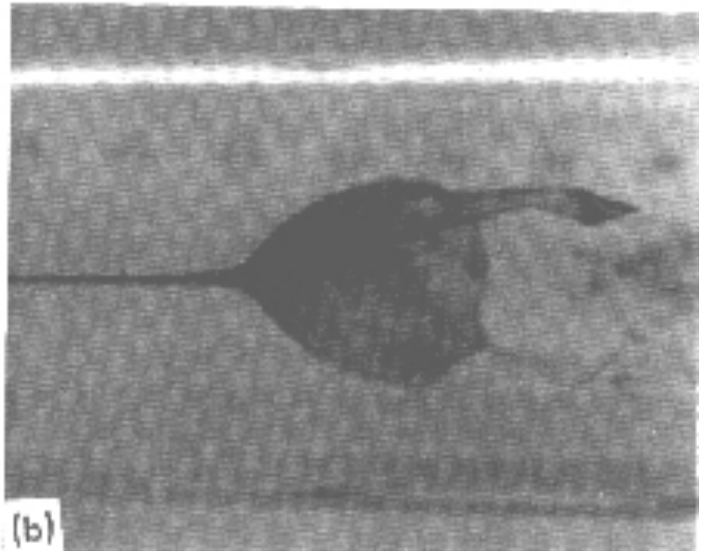

A **Type 4** flattened bubble viewed from the horizontal direction (upper) and the vertical direction (lower).

Flattened Bubble

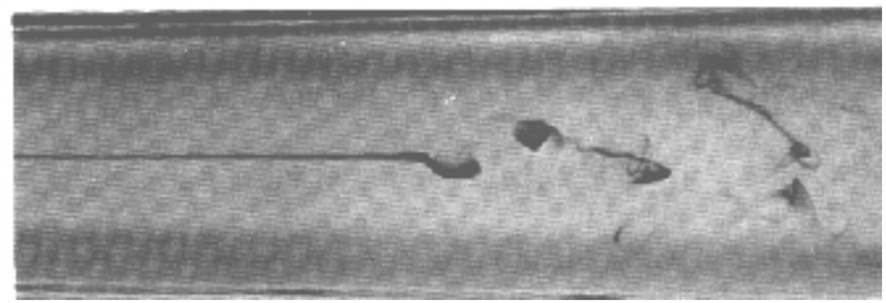

Re = 750, S = 7.5 (Khoo *et al.*).

Conical Breakdown- 8th form?

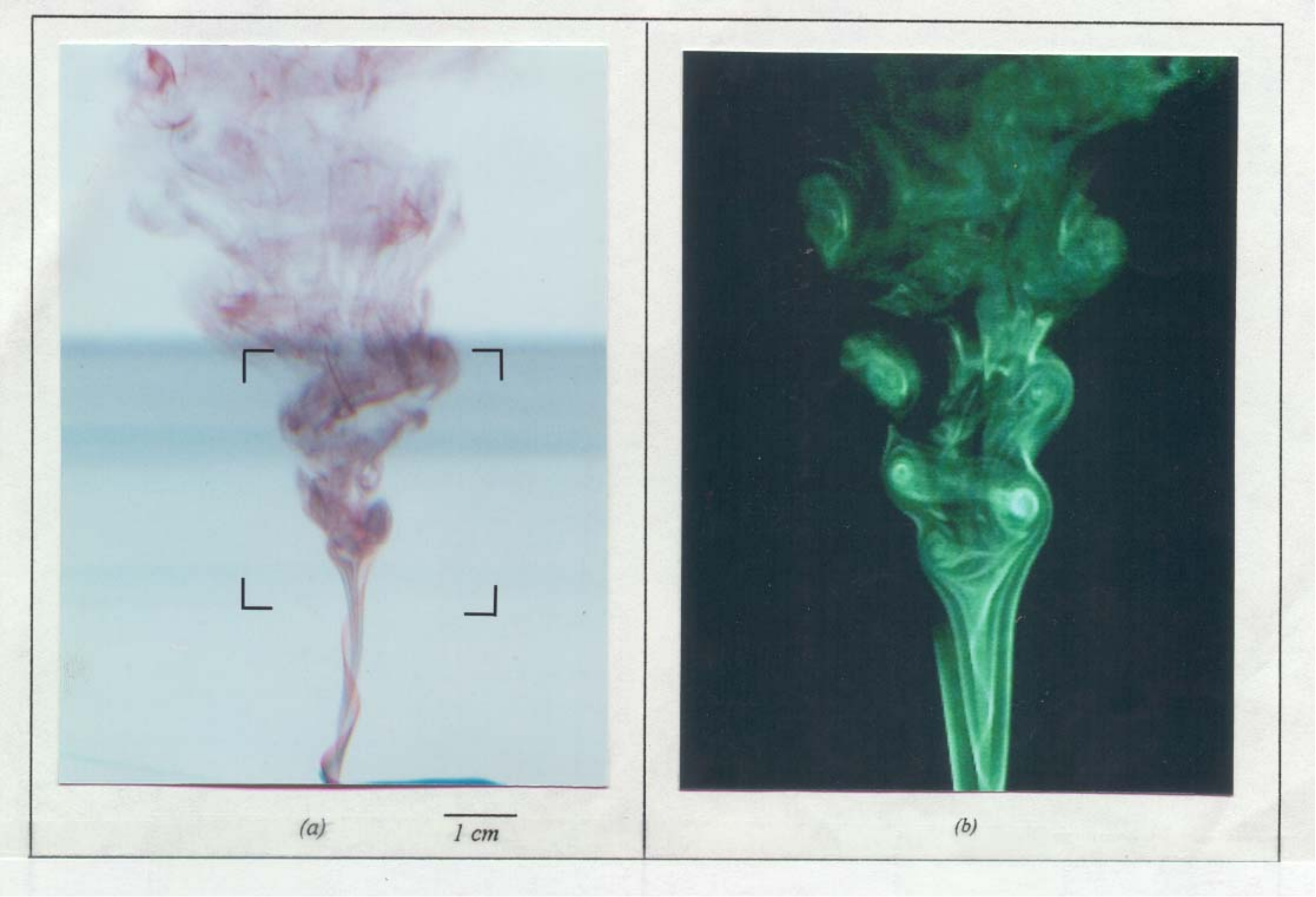

Re = 3500, S = 6.0. (a) Cross-sectional view of the breakdown and (b) close-up (Khoo *et al.*)

Principal Conclusions of Faler and Leibovich

• All flow that exhibit vortex breakdown of the "axisymmetric" form (Types 0 and 1) or "spiral" form (Type 2) are supercritical upstream, in the sense of Benjamin.

• Flows that subsequently undergo vortex breakdown are all stable to infinitesimal inviscid disturbances, including axially symmetric as well as non-axisymmetric perturbations.

• Puzzling flow transients first observed by Sarpkaya can be traced to starting or stopping vortices emanating from the airfoil cascade used to generate swirl in the apparatus.

• There are no closed and axisymmetric disturbance patterns in these flows, and "axisymmetric" vortex breakdown is a misnomer that may have led to the over-emphasis of axial symmetry in theoretical work.

Swirling Pipe Flow – VB transitions

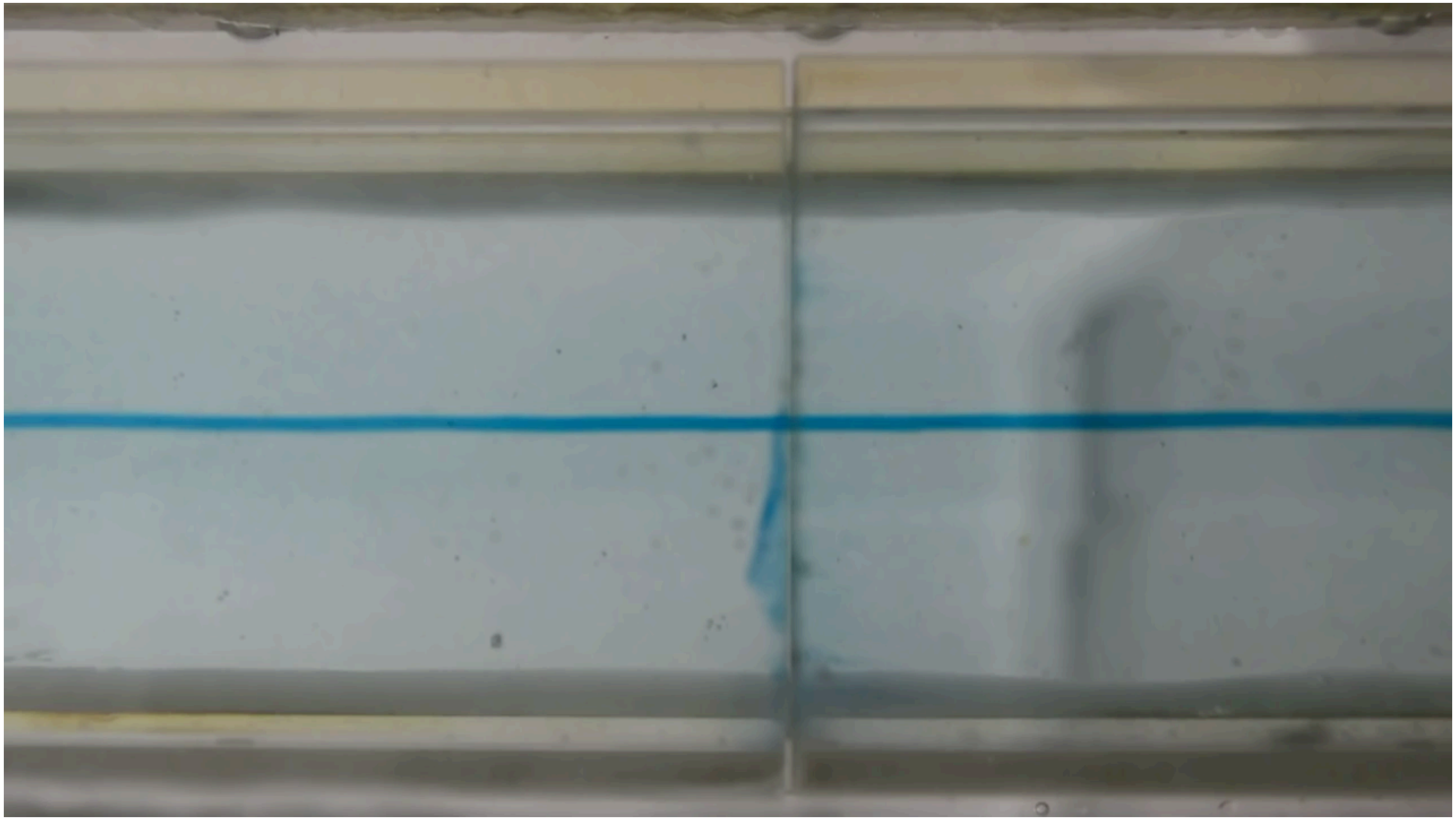

Left half of pipe is rotating, right half stationary. Flow rate constant, rotation increasing with time.
https://www.youtube.com/watch?v=b0TyIlqcEsQ
FERGUL - Fluids Engineering Research Group at the University of Liverpool.

D. J. C. Dennis, C. Seraudie and R. J. Poole "Controlling vortex breakdown in swirling pipe flows: Experiments and simulations". Phys. Fluids 26, 053602 (2014)

Control of Vortex Breakdown - Open Jet

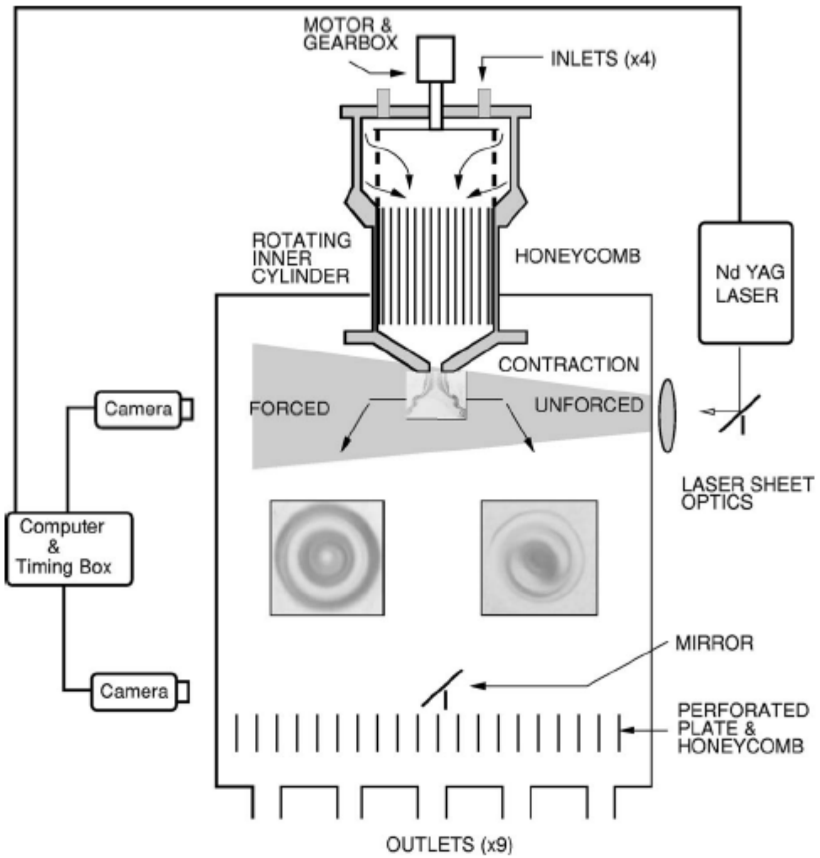

Based on rig of:
Billant, P., Chomaz, J.-M., and Huerre, P. (1998). "Experimental study of vortex breakdown in swirling jets." *Journal of Fluid Mechanics*, **376**, 183-219.

Khalil, S., Hourigan, K. & Thompson, M.C., Effects of Axial Pulsing on Unconfined Vortex Breakdown, Physics of Fluids, 18, 038102, 2006

Basic Structure of Conical Breakdown

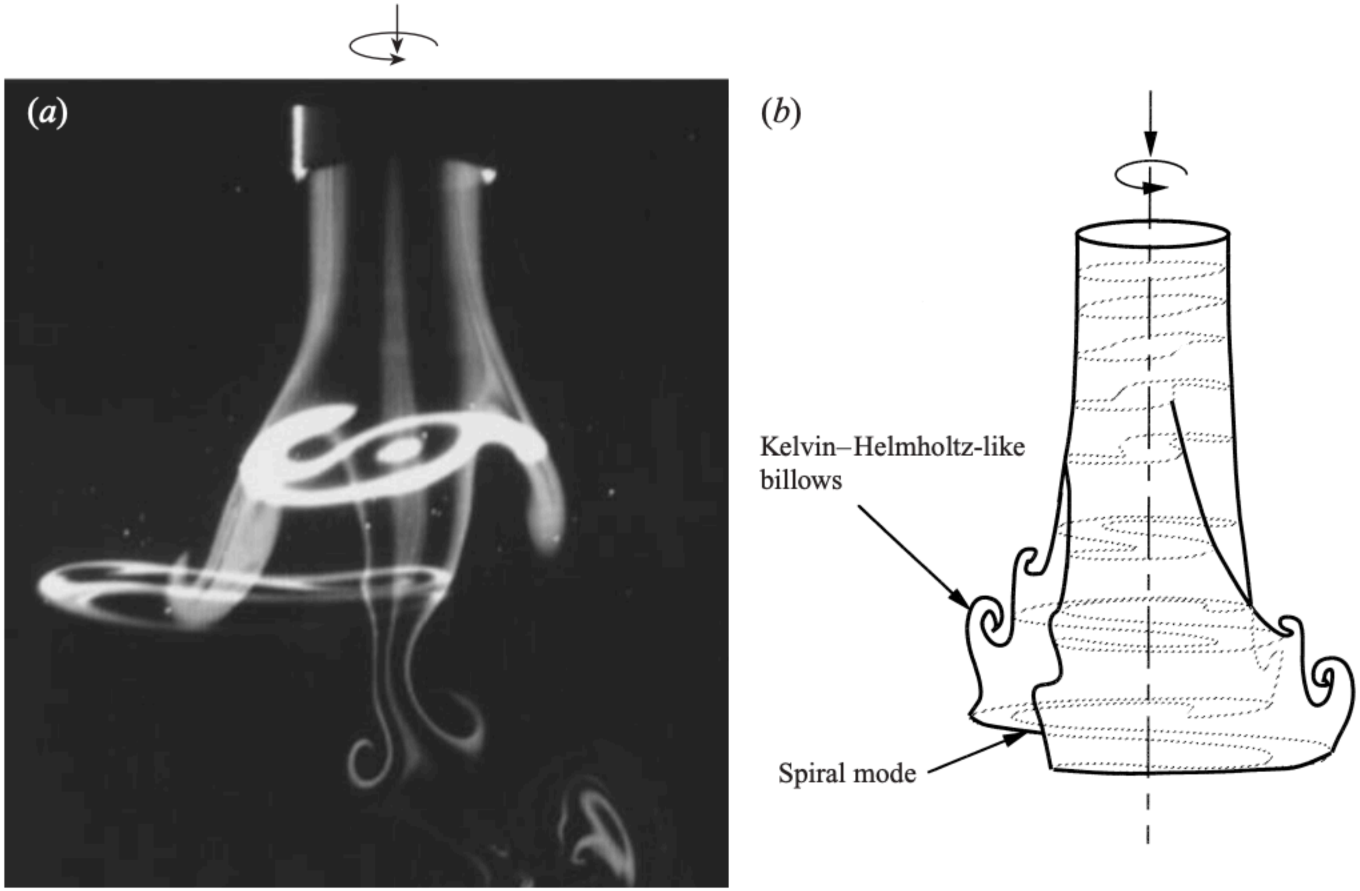

Billant, P., Chomaz, J.-M., and Huerre, P. (1998). "Experimental study of vortex breakdown in swirling jets." *Journal of Fluid Mechanics*, **376**, 183-219.

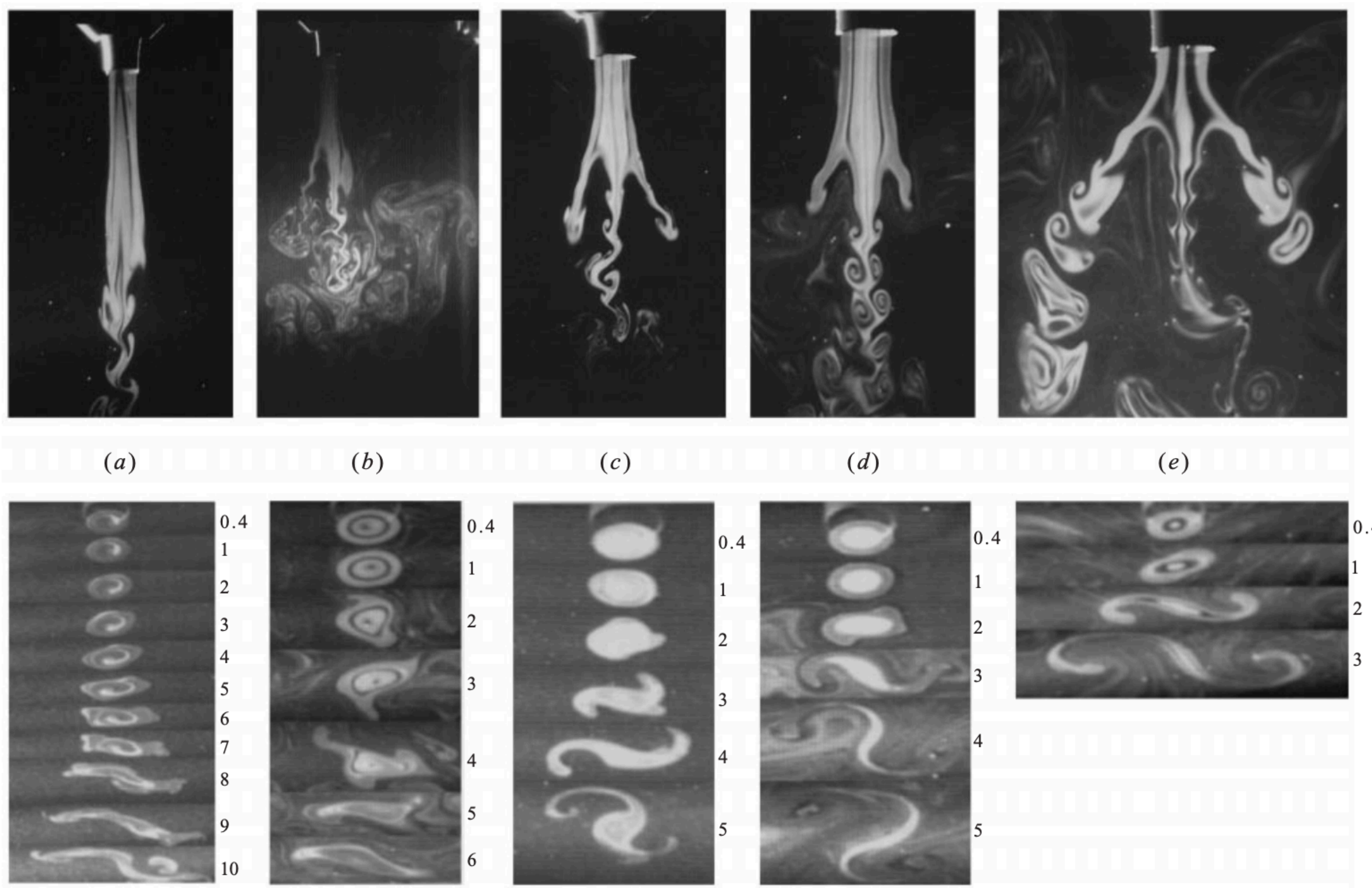

Re = 633 and increasing values of Swirl S

Billant, P., Chomaz, J.-M., and Huerre, P. (1998). "Experimental study of vortex breakdown in swirling jets." *Journal of Fluid Mechanics*, **376**, 183-219.

Control of VB by Axial Pulsation

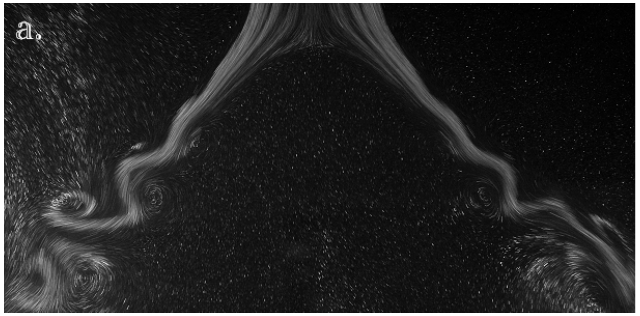

Re=600

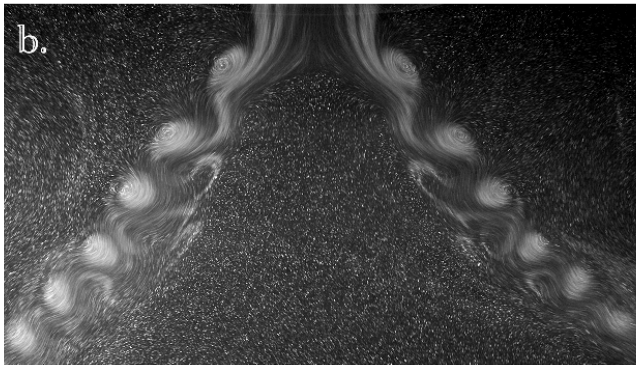

(a) Unpulsed breakdown mυ=0 at, Swirl No. S =1.41

(b) Pulsed breakdown mυ=6%, St=0.78 at Re=600, S=1.41 clearly showing increased vorticity concentrations in the shear layer.

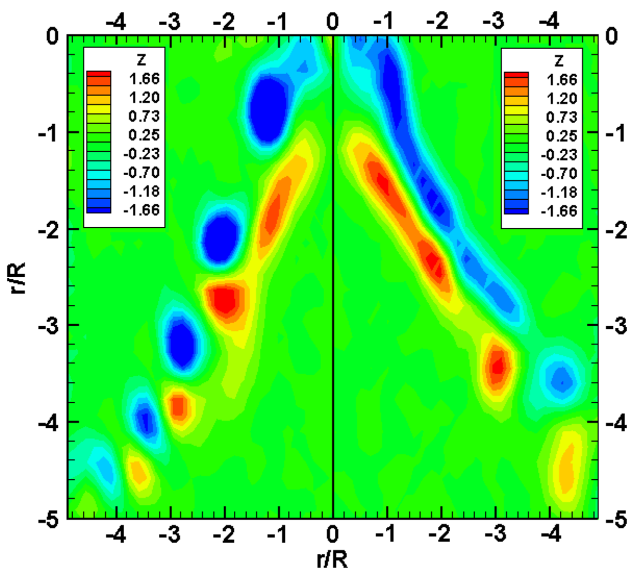

Comparison of pulsed on the left and unpulsed right

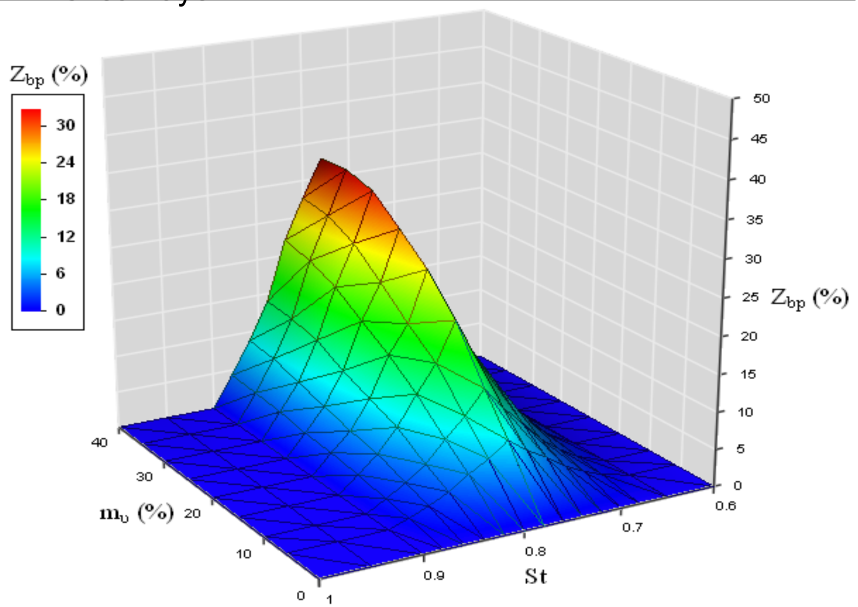

Response of VB to Re=900 S =1.4: change in breakdown position.

Control of VB by Thermal Effects

ΔT = 0°C

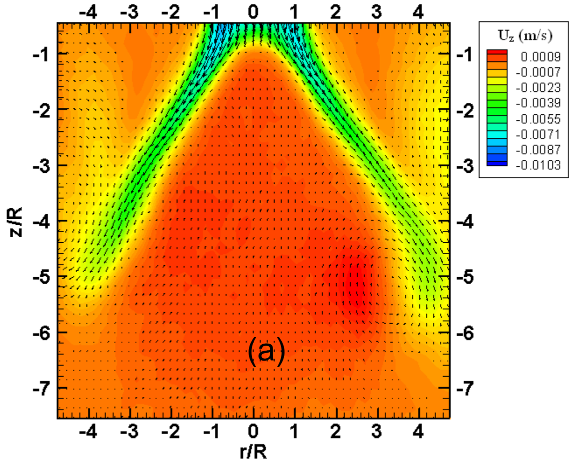

ΔT = 0.5°C

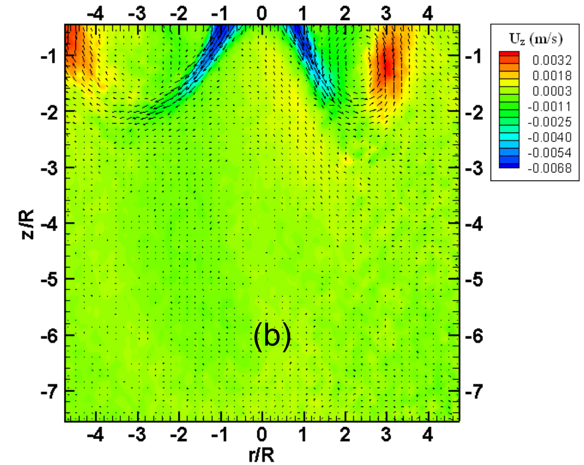

ΔT = -0.5°C

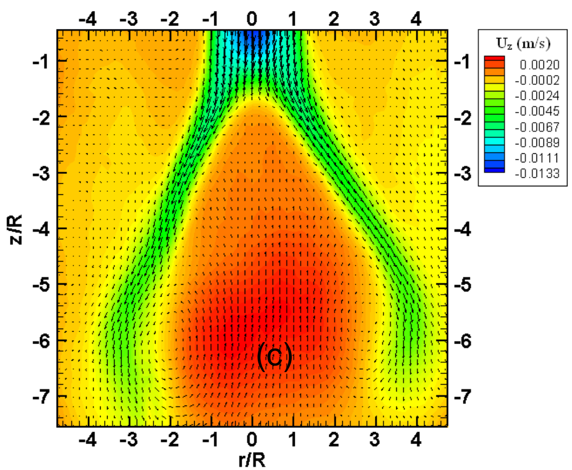

ΔT = -1°C

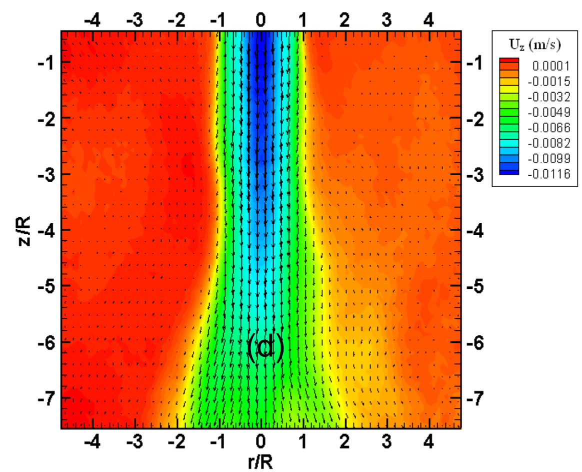

Figure 4.15: SPIV vector and U_z contour plots at Re = 300 and S = 1.35 at (a) ΔT = 0°C, (b) ΔT = 0.5°C, (c) ΔT = -0.5°C and (d) ΔT = -1°C.

Comparison of open and closed flows

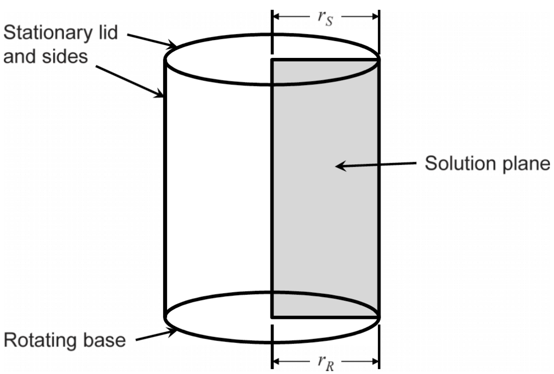

$$Re = \frac{\dot{\Theta} r_R^2}{\nu}.$$

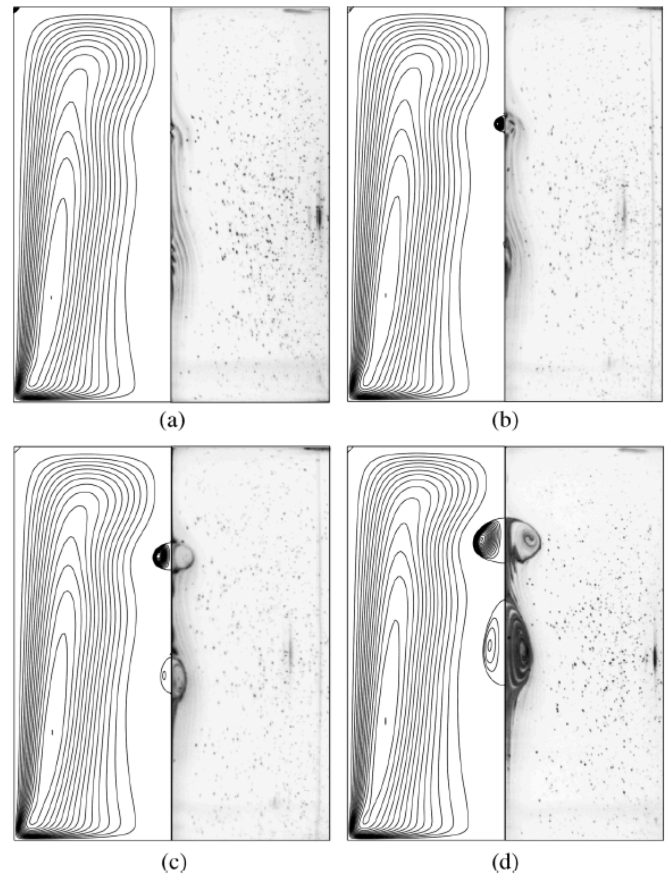

FIG. 2. Numerical versus experimental results for (a) $Re = 1902$, (b) $Re = 1933$, (c) $Re = 2001$, and (d) $Re = 2252$. Experimental dye visualisation taken at the CSIRO by Dr. L. Graham (see Hourigan, Graham, and Thompson[34] for description

Jones, M., Hourigan, K. & Thompson, M.C., A study of the geometry and parameter dependence of vortex breakdown, Physics of Fluids, 27, 044102, 2015.

Hysteresis: Occurs in Open Flows but not Closed Flows?

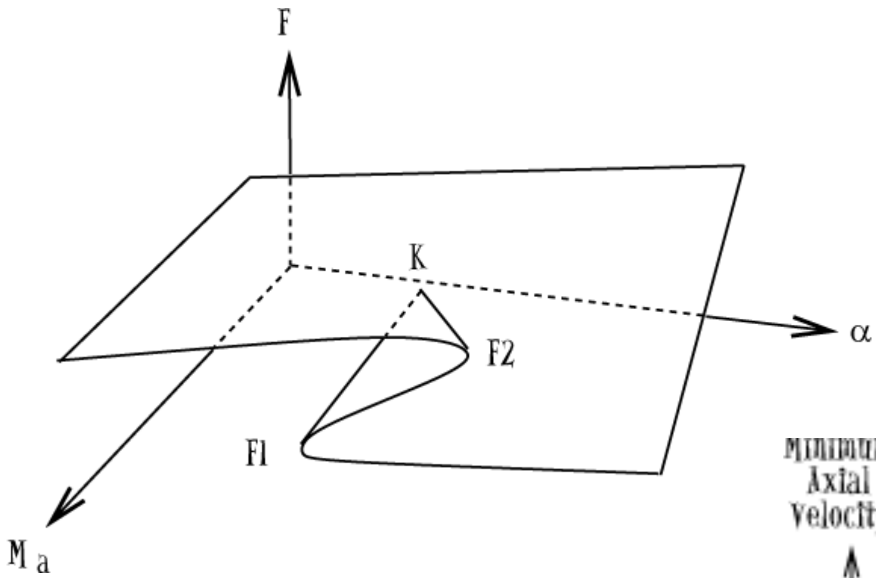

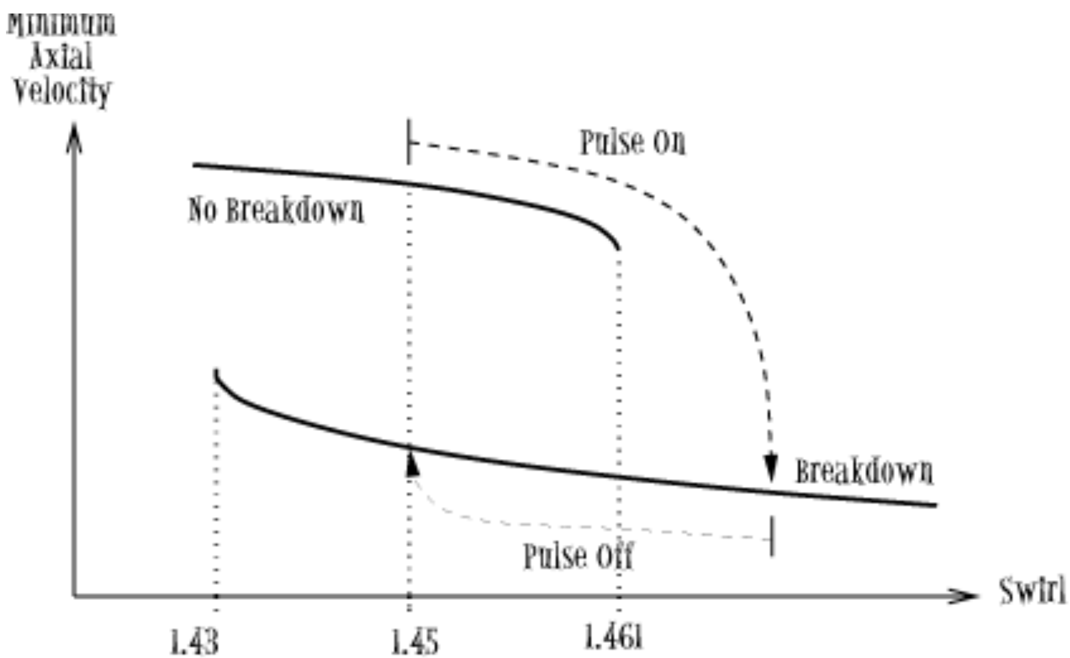

CFD of Open Pipe Flow (based on Faler & Leibovich)

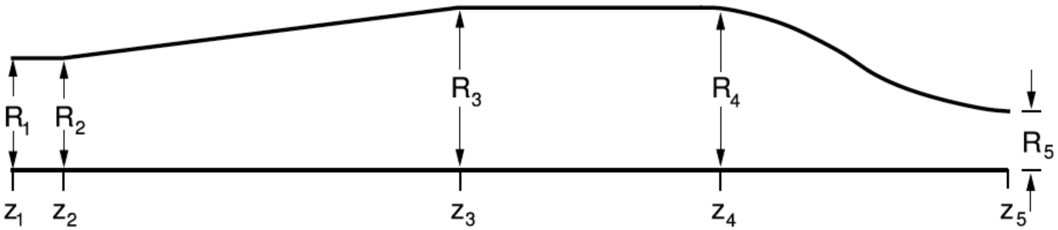

Define Reynolds number and Swirl Parameter based on value and location of max flow velocities for comparison of open and closed flows.

$$Re' = \frac{u_{\max} r_c}{\nu},$$

$$\Omega' = \frac{w_{\max}}{u_{\max}}.$$

u_{max} is the max axial velocity

w_{max} is max azimuthal velocity (on radial line out from location of u_{max})

r_c is radial location of w_{max}

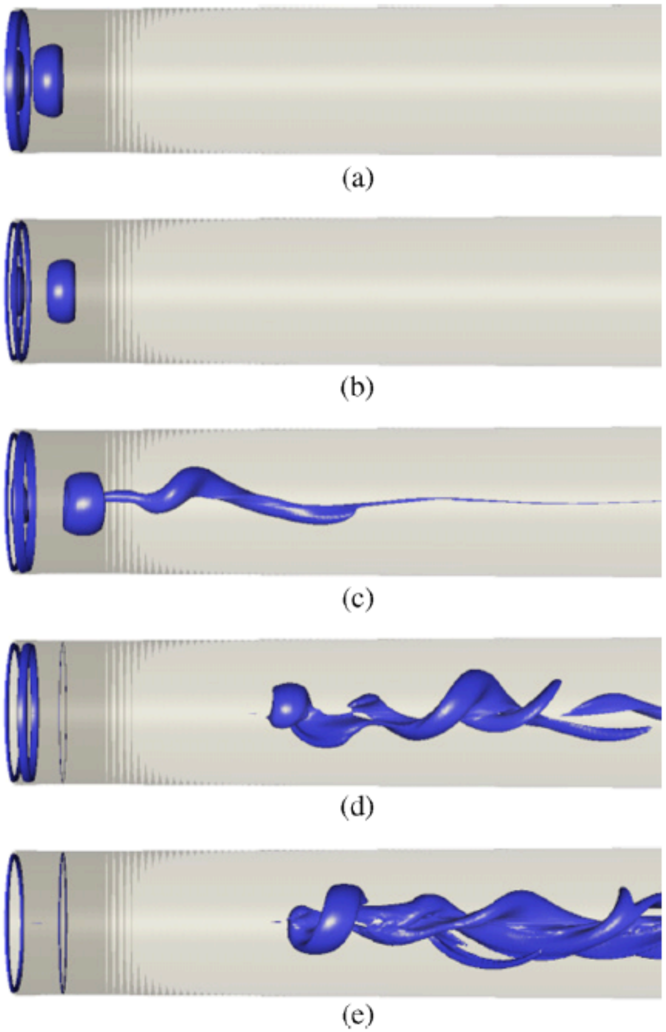

FIG. 6. Results for (a) $Re' = 832$, $\Omega' = 0.668$, (b) $Re' = 416$, $\Omega' = 0.668$, (c) $Re' = 208$, $\Omega' = 0.793$, (d) $Re' = 104$, $\Omega' = 0.919$, and (e) $Re' = 52$, $\Omega' = 1.169$. To visualize the vortical structures, we plot the region where the median eigenvalue λ_2 of the term $S^2 + \Omega^2$ is negative, where S and Ω are the symmetric and antisymmetric parts of the velocity gradient tensor (Jeong and Hussain[57]).

CFD of Open Pipe Flow (based on Faler & Leibovich)

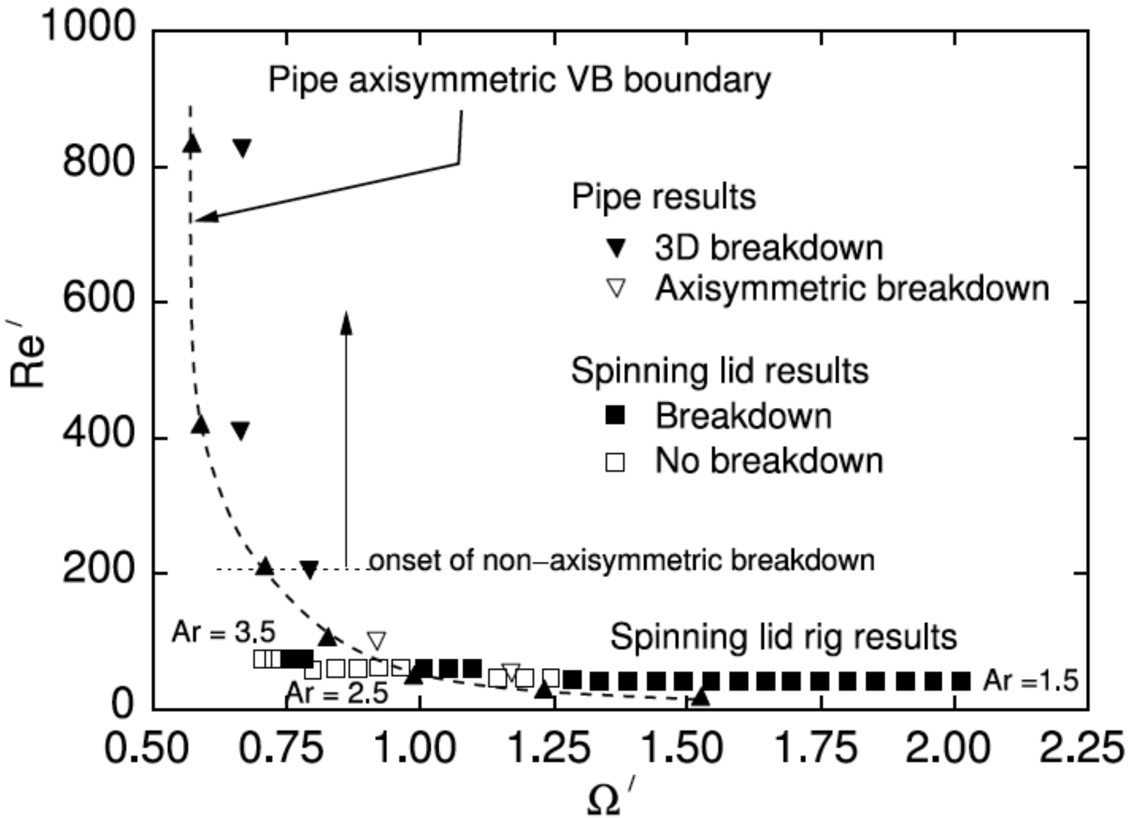

$$Re' = \frac{u_{\max} r_c}{\nu},$$

$$\Omega' = \frac{w_{\max}}{u_{\max}}.$$

FIG. 7. Re' versus Ω' for the TDC (breakdown: □, no breakdown: ■), for the marked aspect ratios. Predictions for the open pipe geometry of Faler and Leibovich[52] are also shown. For the latter case, the dashed line with triangles (▲) indicates the transition curve for steady axisymmetric breakdown obtained from an axisymmetric solver (left: no breakdown, right: breakdown). In addition, inverted triangles show points corresponding to full 3D time-dependent simulations at which breakdown was observed to occur: axisymmetric steady breakdown (▽); non-axisymmetric unsteady breakdown (▼).

Closed Cylinder case occupies a low Re region

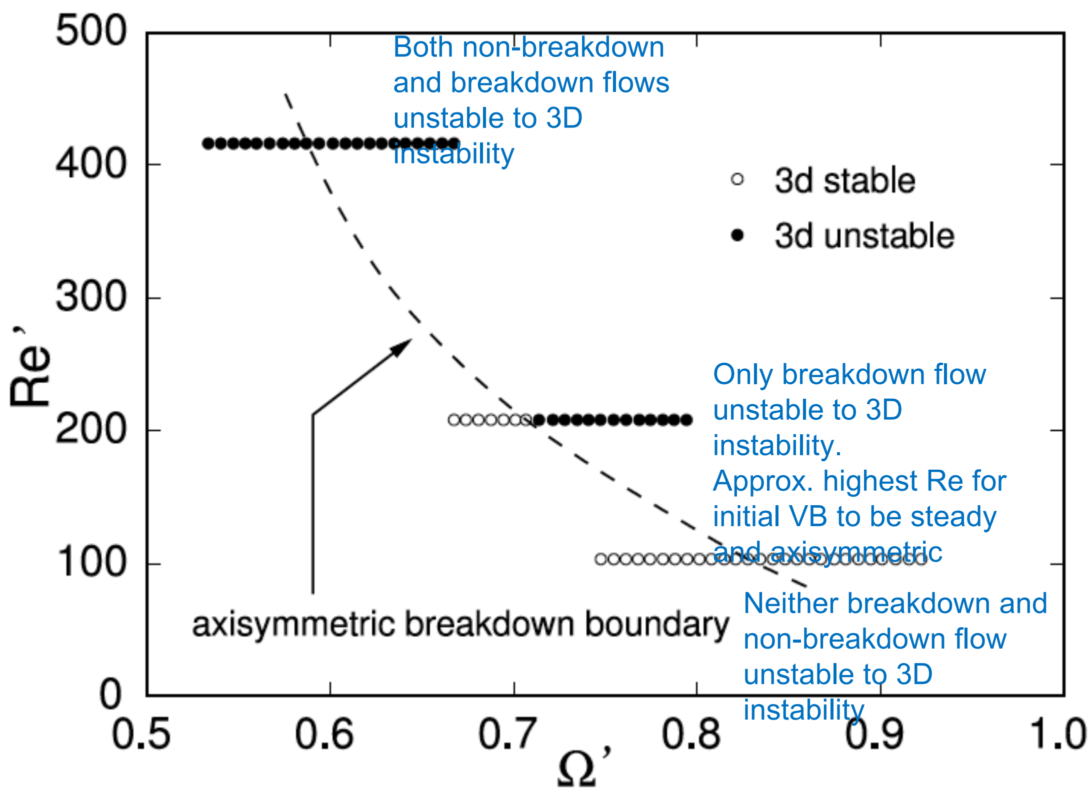

FIG. 8. Stability of steady axisymmetric flow state to three-dimensional perturbations for the pipe geometry of Faler and Leibovich.[49]

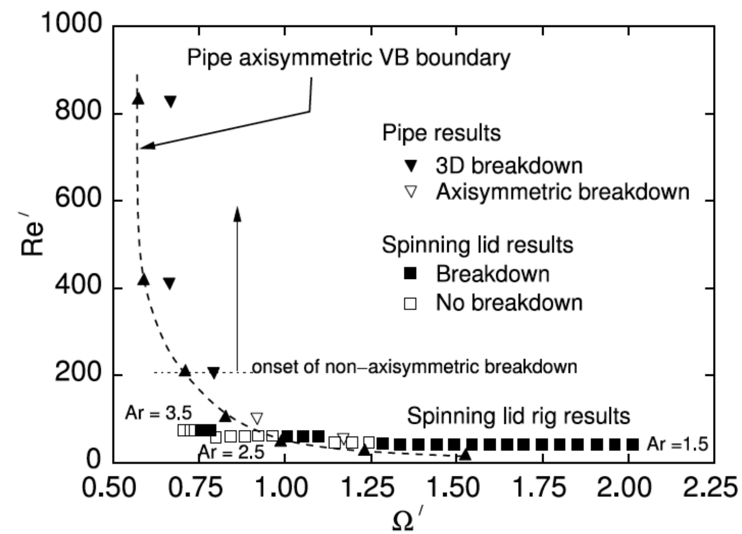

Closed cylinder: cannot get Re' above about 100, so do not see spiral breakdown.

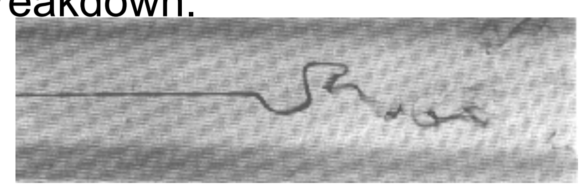

Previous Experiment of a Sphere in Swirling Tube

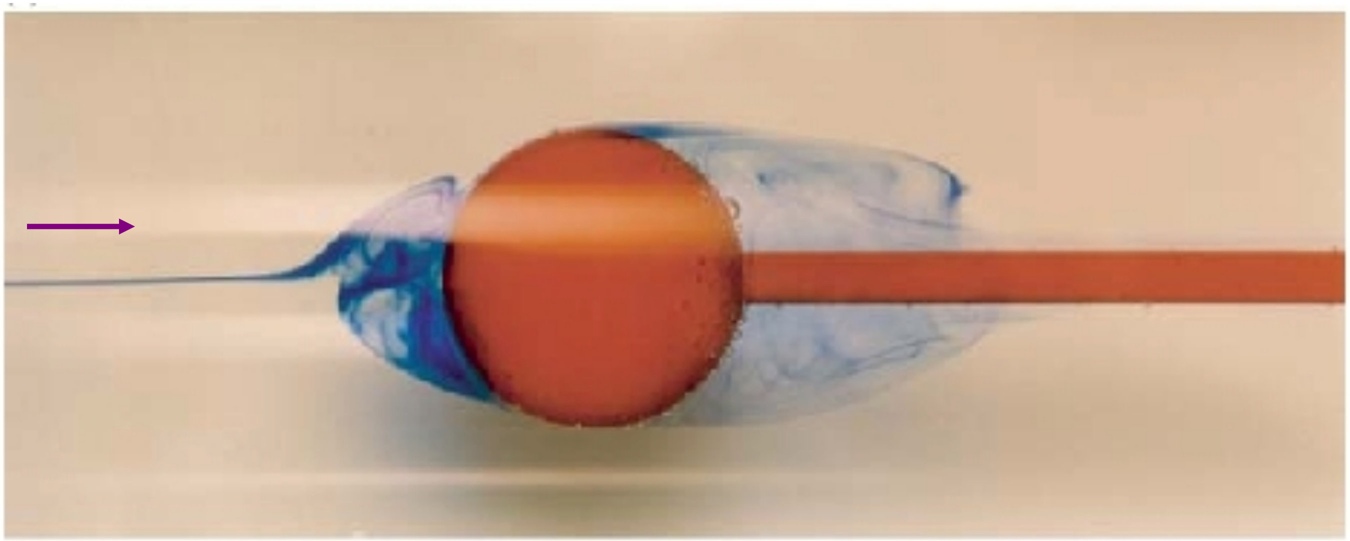

Mattner, T.W., Joubert, P.N. and Chong, M.S.
"Vortical flow. Part 2. Flow past a sphere in a constant-diameter pipe"
J. Fluid Mech (2003), v481, pp1-36

Open Jet Swirling Flow: sphere on axis

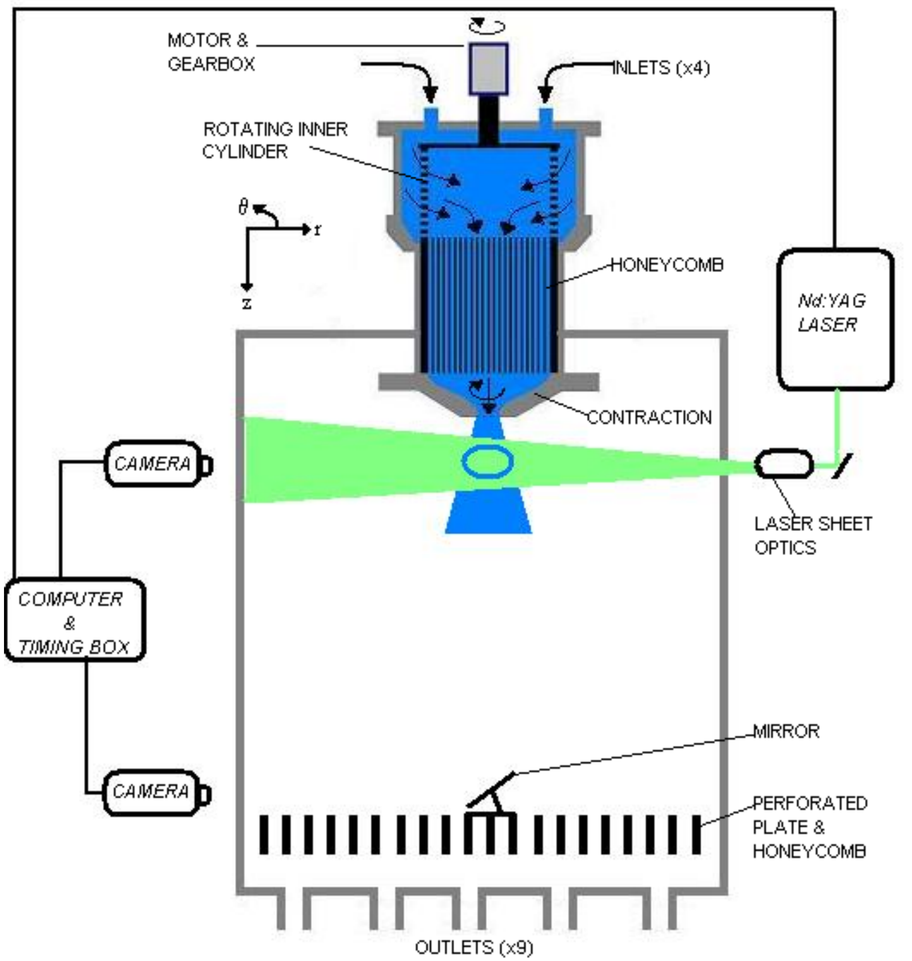

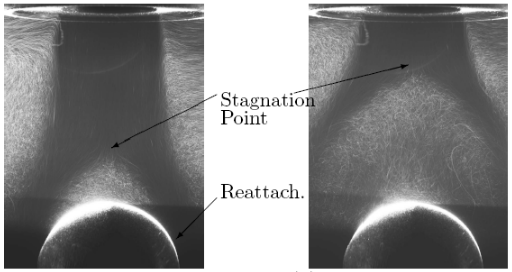

(a) Closed state, at $Re_\omega = 253$ (b) Open state, at $Re_\omega = 257$

Figure 3. Comparison between (a) a closed recirculation zone between the sphere surface and the stagnation point, with the vortex breakdown shear-layer re-attaching to the sphere surface, and (b) an open form of breakdown, with shear-layer clear of sphere surface. Images are taken for $Re_x = 750$, and $D_S = 1.47 \pm 0.02$, $x_S = 1.99 \pm 0.03$.

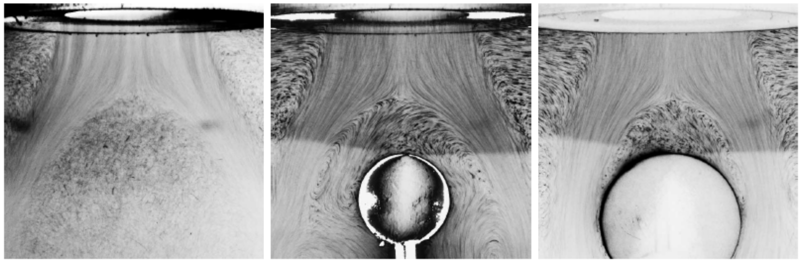

(a) No Sphere (b) $D_S = 0.62$ (c) $D_S = 0.97$

Figure 5. Flow visualisation of the same stagnation point location for the cases of (a) no-sphere at $S_K = 9.6$, (b) $D_S = 0.62$ at $S_K = 9.7$ and (c) $D_S = 0.99$ at $S_K = 10.3$. The shear-layer of the vortex breakdown region for the larger sphere is attached to the sphere surface but open for the smaller sphere, as for the no-sphere case. Images taken at $Re_x = 600$.

Base Case: No sphere

Re_x : 450, 600, 750, 900

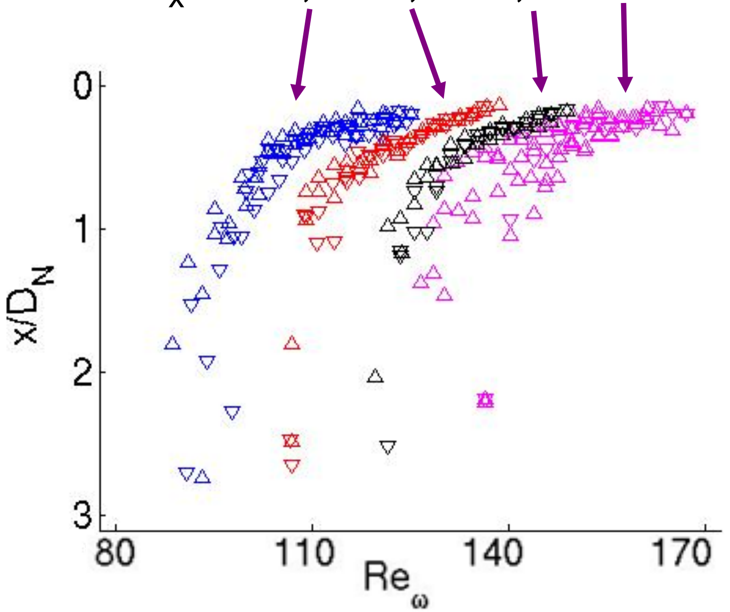

Stagnation point position vs Swirl Number

Sphere

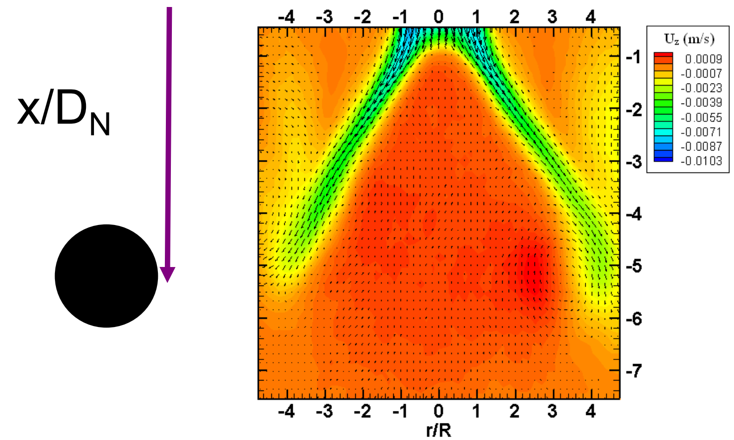

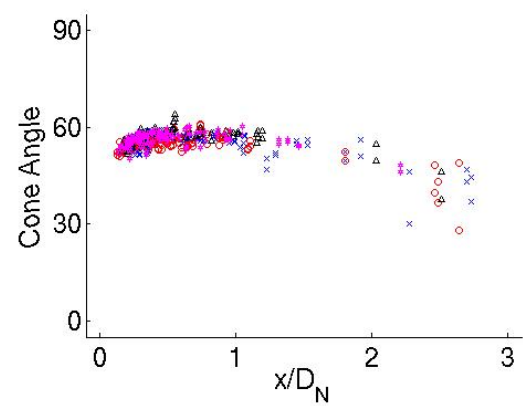

Cone angle vs Position of Sphere

Sphere Case: $x_{sphere} = D_{sphere} = D_{Nozzle}$

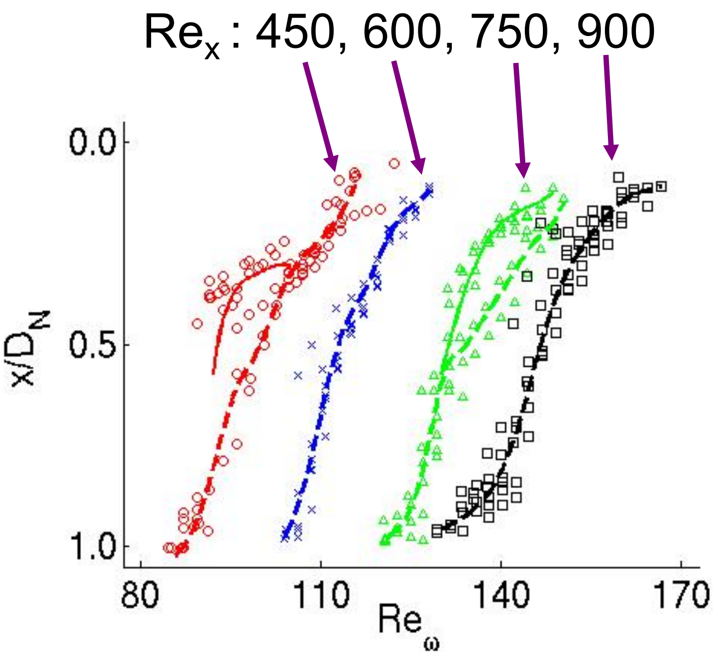

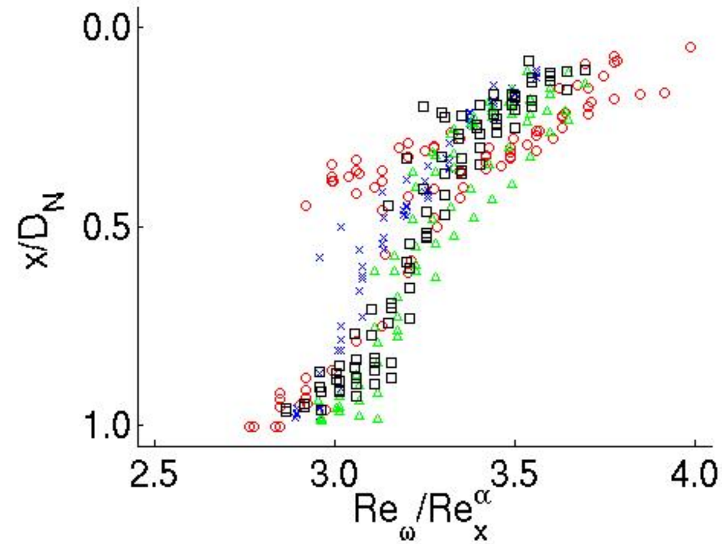

Best collapse (α = 0.56)

Vortex ring versus vortex breakdown

Moderate strength vortex ring

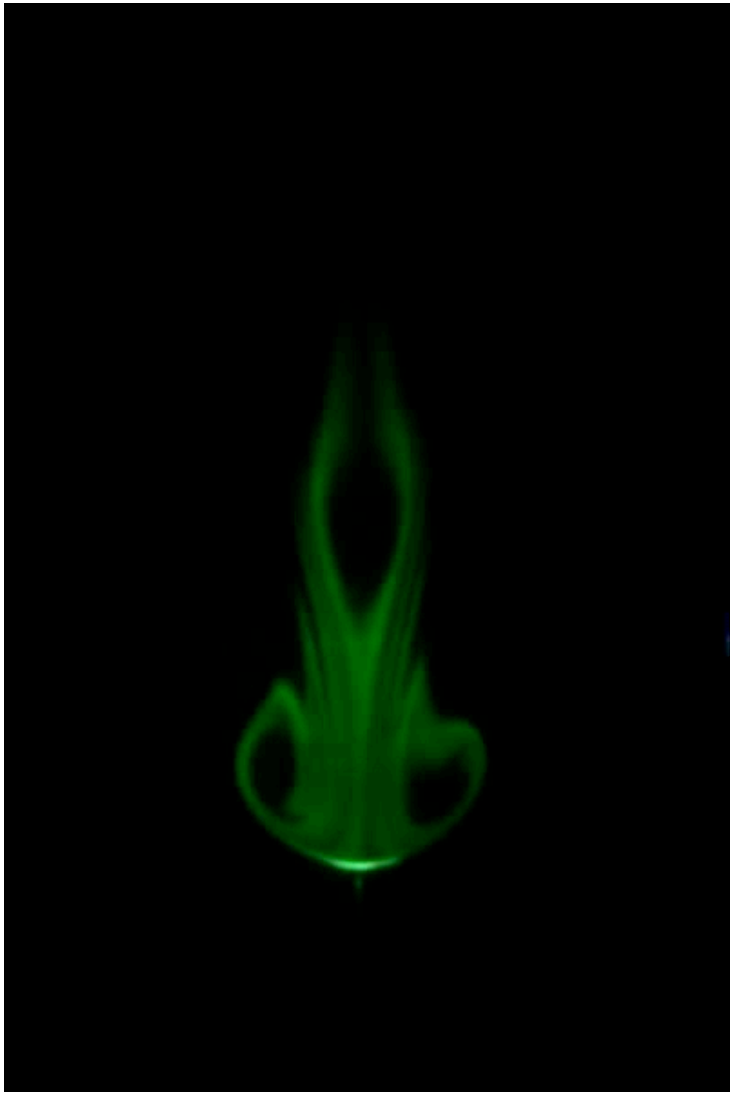

Vortex ring versus vortex breakdown

High strength vortex ring

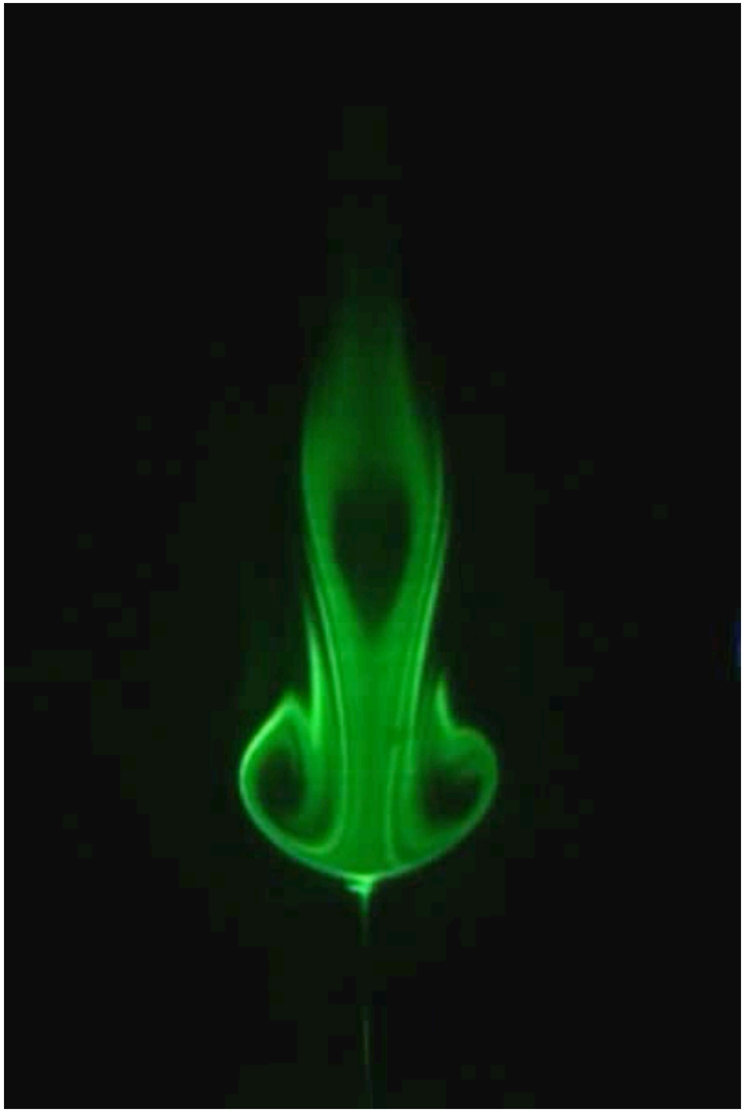

Conclusions

Swirling jet in an open flow or pipe

- Many different types of vortex breakdown observed

- Fundamentally similar to the closed cylinder breakdown, which is constrained usually to much lower Reynolds numbers

- Effects of a bluff body on the vortex breakdown
  - Size and position of VB bubble shown to be influenced by axial pulsation, thermal effects and presence of sphere along axis